IMPERIAL COLLEGE LONDON

Department of Earth Science and Engineering

Centre for Petroleum Studies

Design of a Pressure Transient Campaign for a Giant Middle Eastern Field

By

Ali Izzidien

A report submitted in partial fulfilment of the requirements for the MSc and/or the DIC.

September 2012

DECLARATION OF OWN WORK

I declare that this thesis

Design of a Pressure Transient Campaign for a Giant Middle Eastern Field

is entirely my own work and that where any material could be construed as the work of others, it is fully cited and referenced, and/or with appropriate acknowledgement given.

Signature:.....

Name of student: Ali Izzidien

Name of supervisor: Professor Alain C. Gringarten

Name of the company supervisor: James Boyle

Acknowledgements

I would like to thank the field operators for providing the opportunity to conduct this study, and permission to publish its results.

I am grateful for the guidance provided by my supervisors Prof. Alain Gringarten (Imperial College London) and James Boyle, as well as all the staff working for the field operator who have provided considerable guidance at various stages in this project.

I would like to express my gratitude to Petrofac and The Royal Academy of Engineering for providing a fellowship which has supported me during this degree programme.

Finally, I would like to thank all my friends, family, and mentors for providing their support and council in my decision to pursue a career as an engineer. In particular I would like to thank K. Imam, M. Alshawaf, and S. Saxena.

Table of Contents

List of Figures

List of Figures – Appendices

List of Tables

List of Tables - Appendices

Imperial College London

MSc in Petroleum Engineering 2011-2012

Design of a Pressure Transient Campaign for a Giant Middle Eastern field

Ali Izzidien

Professor Alain C. Gringarten, Imperial College

James Boyle, Field Operating Organisation

Abstract

Pressure Transient Analysis has been used for many years to establish well and reservoir parameters. The practice of shutting in wells for Pressure Build Up or Pressure Fall Off analysis has often made this unpopular with operators wishing to avoid lengthy production curtailment. The objective of this study is to provide guidelines for minimum build-up durations in a giant Middle Eastern field through analysis of a number of wells. This paper also presents a method which allows Pressure Transient Analysis to take place without shutting a well.

When operating large onshore fields, the capital expenditure and production curtailment associated with installing permanent down-hole gauges in wells post-completion makes them difficult to justify. In many such fields, a large proportion of wells already operate using Electrical Submersible Pumps. In most cases these pumps record inlet pressures, but the quality of this data is generally poor. Using simulated data, this study demonstrates that analysis is possible even with low quality data (10psi resolution) provided the data quality is compensated by data quantity.

Introduction

Shutting in of wells for the purpose of Pressure Transient Analysis (PTA) in the field being reviewed is currently limited to situations where it is deemed essential to ensure a well continues to produce. This is primarily due to management concerns over production curtailment. The current process is to shut in wells for 24-36 hours. With some wells achieving over 10,000bpd, this can equate to revenue losses in excess of $1 million.

By performing PTA on six wells from the field, the objective of this study is to provide guidelines for minimum build-up durations for that field to ensure that all pertinent data is collected, while avoiding unnecessary production losses.

A second objective is to investigate the feasibility of performing Pressure Transient Analysis (PTA) of low quality, variable flow rate pressure data collected from Electrical Submersible Pump (ESP) pressure gauges using deconvolution. Deconvolution of pressure data at variable flow rate from permanent downhole gauges is well established in the literature (von Schroeter *et al*., 2002; Levitan *et al*., 2006). Specific goals of this study are threefold:

- To put limits on data errors quantified by previous authors into the context of ESP data, specifically to identify the minimum acceptable pressure resolution
- To propose a method for overcoming the data quality constraints suggested by previous authors
- To investigate how a reduced sampling frequency affects deconvolution

Field Overview

The field comprises two giant domes in pressure communication and separated by a saddle. There are two distinct formations constituting separate reservoirs across both domes, The Sandstone, and The Limestone. Fig. 1 shows a summary of the field, together with the locations of the wells for which pressure transient data has been analysed.

The Sandstone comprises a highly layered deltaic stratigraphy. It is composed of sheets of excellent quality channel sands (100-5000mD) in the South, together with moderate quality shoreline sands (10-100mD), and silt and shale deposits. Shoreline sands are flooded leading to extensive shale depositions. Channel sands are deposited into areas where the underlying formation has been significantly eroded. The majority of shale deposits are localised, with the exception of two extensive layers which split the reservoir vertically into zones A, B and C. The Sandstone has strong aquifer support within the southern dome, but this is augmented by water injection in the northern dome where it is significantly weaker.

The Limestone is composed of a massive clean limestone, with some shale. The southern dome porosity is marginally superior to the North. The northern dome is considered of greater quality due to a 100mD average permeability interlaced with frequent 300mD streaks. This is in contrast to the south where permeability below 30mD has caused development to be avoided. The Limestone has a weak aquifer, but pressure maintenance is almost entirely from water injection.

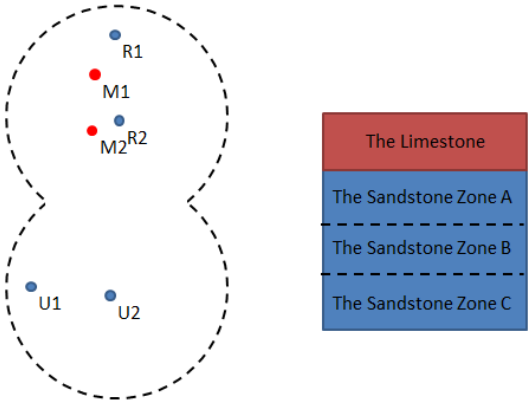

Fig. 1: Summary of well locations

Well U1

Well U1 is a producer situated on the western flank of the southern dome, and is perforated within zone B of The Sandstone. PTA has been performed on a 39 hour shut-in which occurred during flow performance tests following 3 months of production.

The well is interpreted as having limited entry and being in a closed reservoir due to no-flow interference boundaries caused by surrounding wells (Fig. 2). Table 1 and Fig. 3 show the results of the analysis from which the following points are highlighted:

- Interpreted permeability of 2355 is significantly higher than the 700mD estimated from log analysis
- 75% of skin appears to be mechanical in nature
- The drainage area extends 4800ft to the north east due to interference boundaries, possibly providing an opportunity for infill drilling
-

Table 1: Well U1 PTA interpretation

Simulation Data	Partial Penetration Well
Well. storage	0.07 bbls/psi
Skin(mech.)	8.6
Permeability	2355mD
Kv/Kh	1
Eff. Thickness	78feet
Zp/Heff	0.5
Skin(Global)	11.4
Perm-Thickness	184000. mD-ft
+x boundary	2400. feet (No Flow)
-x boundary	1300. feet (No Flow)
+y boundary	4200. feet (No Flow)
-y boundary	1500. feet (No Flow)
Initial Press.	5567.2 psi
Deconv. Initial Press.	5567.2 psi
Model Pore-Volume	.5300e+09 feet^3
Model Ct	.1253e-04 1/psi
Conditioning Coeff.	0.01
Obj.Func.	1412.7
Initial Press.	5567.2 psi
Datum Press.	4648.1 psi
Average Press.	4648.1 psi
Smoothing Coef	0.030,0.030

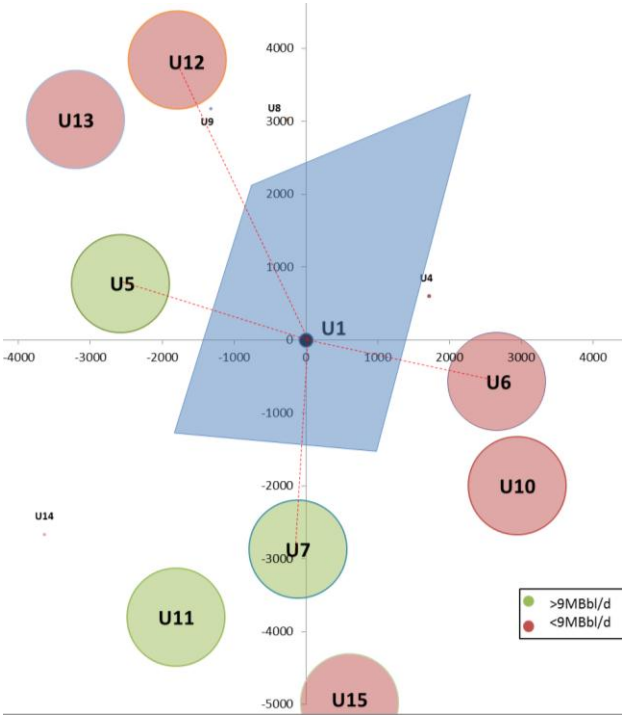

Fig. 2: Well U1 proximity to neighbouring wells, and influence on interference boundaries

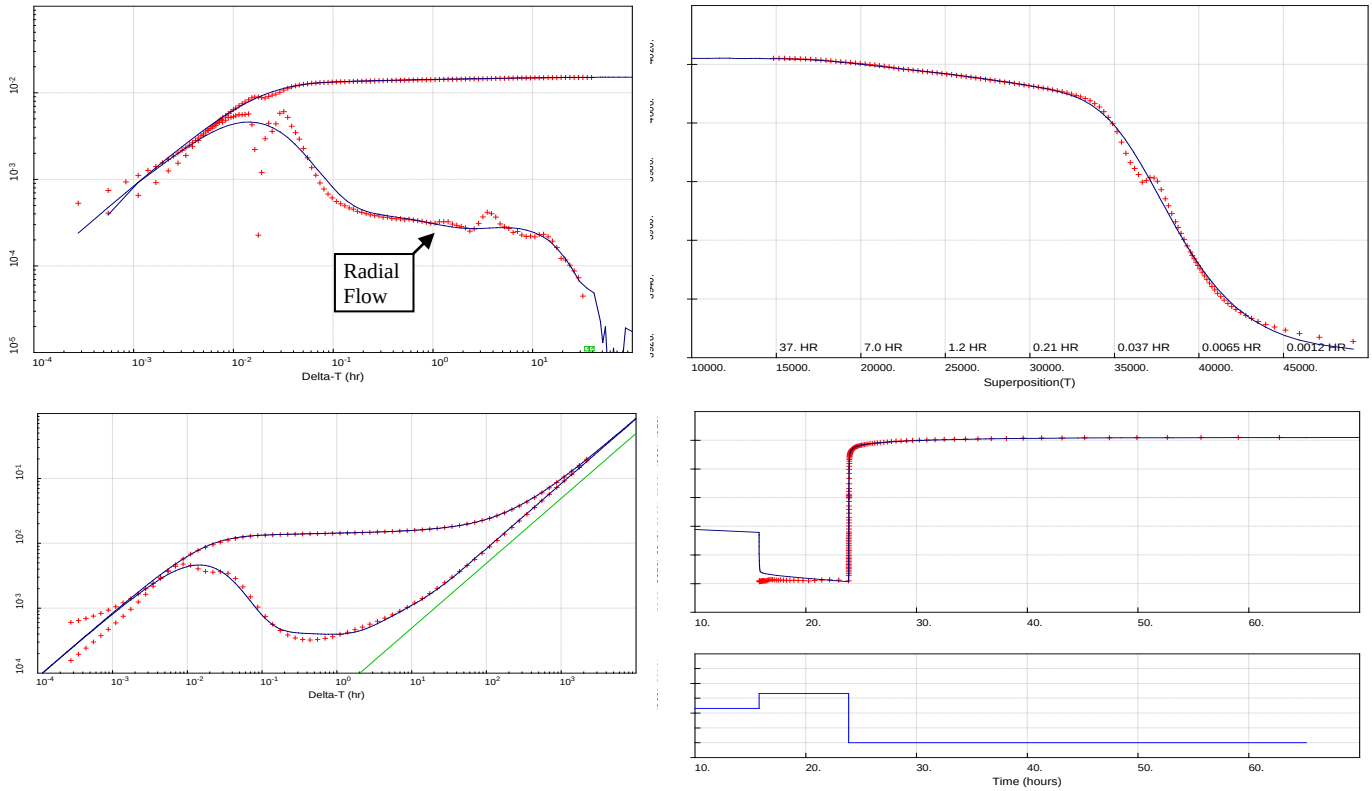

Fig. 3: Well U1 results of interpretation using, clockwise from top left: log-log and derivative analysis, superposition analysis, deconvolution and pressure history match

Well U2

Well U2 is a producer situated towards the crest of the southern dome, with flow from zone B of The Sandstone dominating. PTA has been performed on a 28 hour shut-in which occurred during flow performance tests following 2 months of production.

The well is interpreted as having limited entry and being in a closed reservoir due to interference boundaries caused by surrounding wells (Fig. 4). **Error! Reference source not found.** and Fig. 5 show the results of the analysis from which the following points are highlighted:

- Interpreted permeability of 1200mD is consistent with the 900mD found through log analysis
- Only 20% of skin appears to be mechanical in nature, suggesting that there may be opportunities to enhance production
- The drainage area extends 2800ft to the south-west due to interference boundaries, possibly providing an opportunity for infill drilling

Table 2: Well U2PTA interpretation

Simulation Data	Partial Penetration Well
Well. storage	0.075 bbls/psi
Skin(mech.)	5.4
Permeability	1200 mD
Kv/Kh	1.60e-04
Eff. Thickness	270 feet
Zp/Heff	0.5
Skin(Global)	27
Perm-Thickness	323950. mD-feet
+x boundary	1000. feet (No Flow)
-x boundary	2500. feet (No Flow)
+y boundary	1100. feet (No Flow)
-y boundary	2800. feet (No Flow)

Initial Press.	4145.8 psi
Datum Press.	3959.2 psi
Average Press.	3726.5 psi
Smoothing Coef	0.,0.
Deconv. Initial Press.	4145.8 psi
Model Pore-Volume	.54e+9 feet^3
Model Ct	.1498e-04 1/psi
Conditioning Coeff.	0.01
Obj.Func.	2433.6

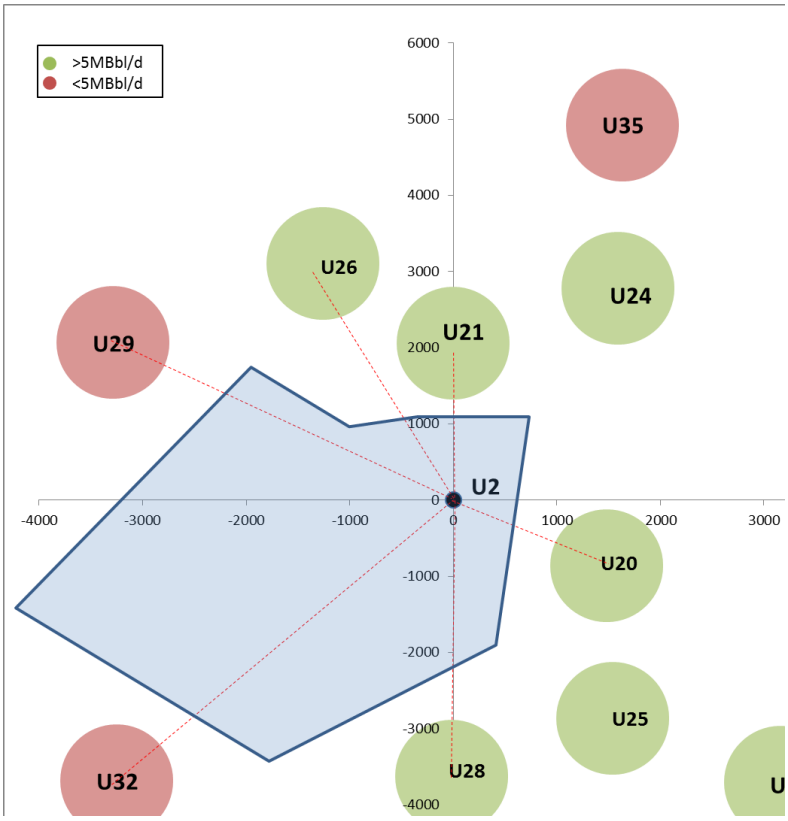

Fig. 4: Well U2 proximity to neighbouring wells, and influence on interference boundaries

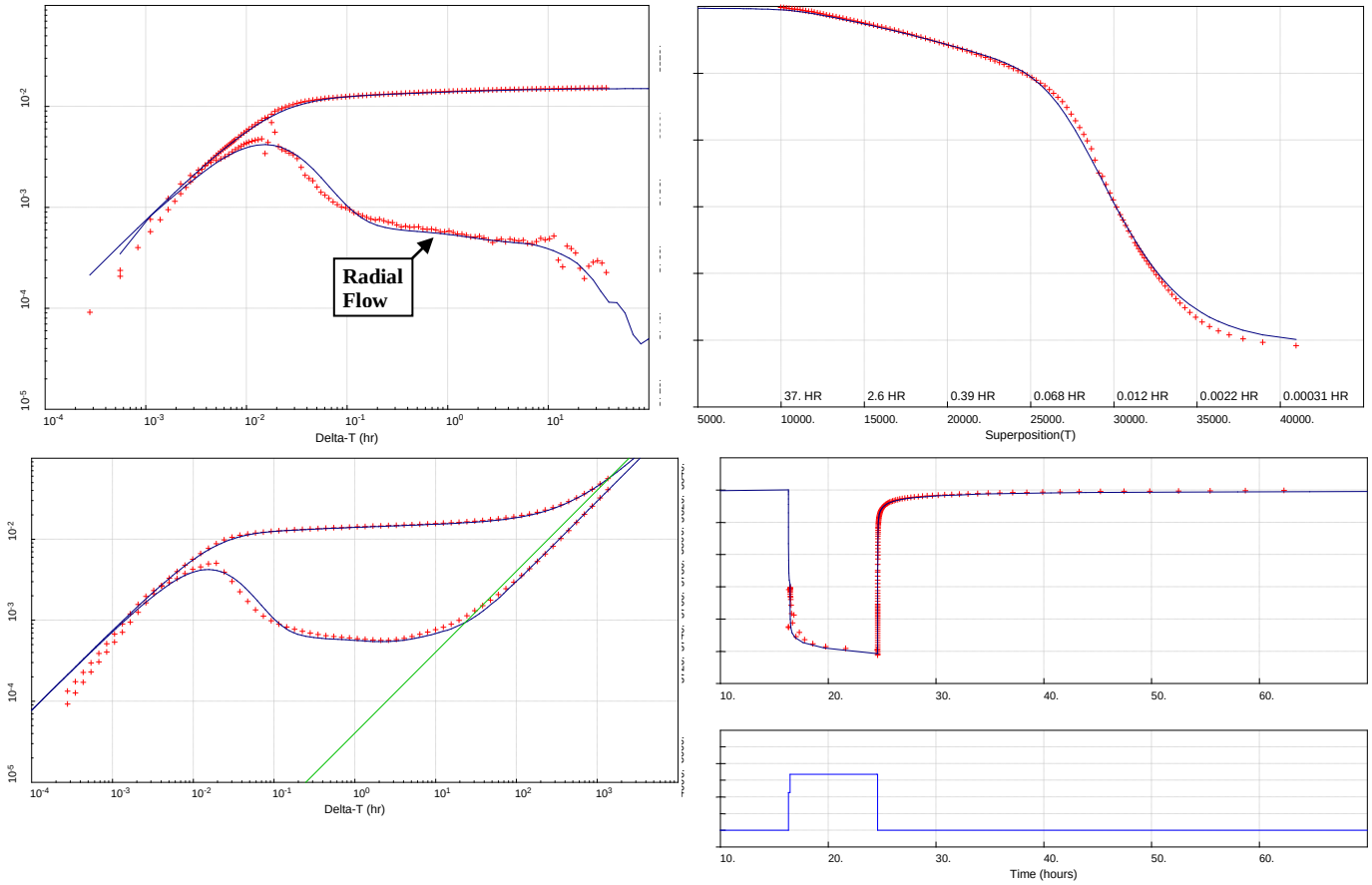

Fig. 5: Well U2 results of interpretation using, clockwise from top left: log-log and derivative analysis, superposition analysis, deconvolution and pressure history match

Well R1

Well R1 is a producer positioned in the northern most quadrant of the northern dome, and perforated in zone C of The Sandstone. Following 6 months of production, the well was shut in twice, first for 32 hours, then for 22 hours, with pressures being recorded using wire-line memory gauges for the second Pressure Build-Up (PBU) only.

The well is interpreted as being close to a fault, and in a closed reservoir due to interference boundaries caused by the proximity of other wells (Fig. 6). Table 3 and Fig. 7 show the results of the analysis from which the following points are highlighted:

- Interpreted permeability of 2100 is considerably higher than the c.150mD found through log analysis, but is geologically consistent with other parts of the northern dome
- Skin of 10.1 suggests there may be opportunities to enhance production from this well
- The drainage area extends 10,000ft to the south-west, possibly providing an opportunity for infill drilling

Table 3: Well R1 PTA interpretation

Simulation Data	homogeneous reservoir
Well. storage	0.06 bbls/psi
Skin	10.1
Permeability	2100 mD
Areal Ky/Kx	2.5
Perm-Thickness	66150. mD-feet
+x boundary	5500. feet (No Flow)
-x boundary	1100. feet (No Flow)
+y boundary	320. feet (No Flow)
-y boundary	10000 feet (No Flow)
Initial Press.	4592.9 psi
Datum Press.	4565.1 psi
Deconv. Initial Press.	4592.9 psi
Conditioning Coeff.	0.01
Obj.Func.	409.5
Initial Press.	4592.9 psi
Smoothing Coef	0.,0.

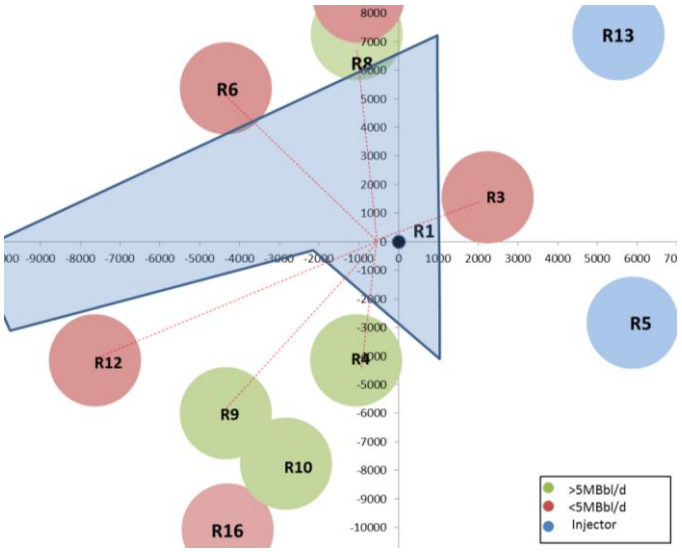

Fig. 6: Well R1 proximity to neighbouring wells, and influence on interference boundaries

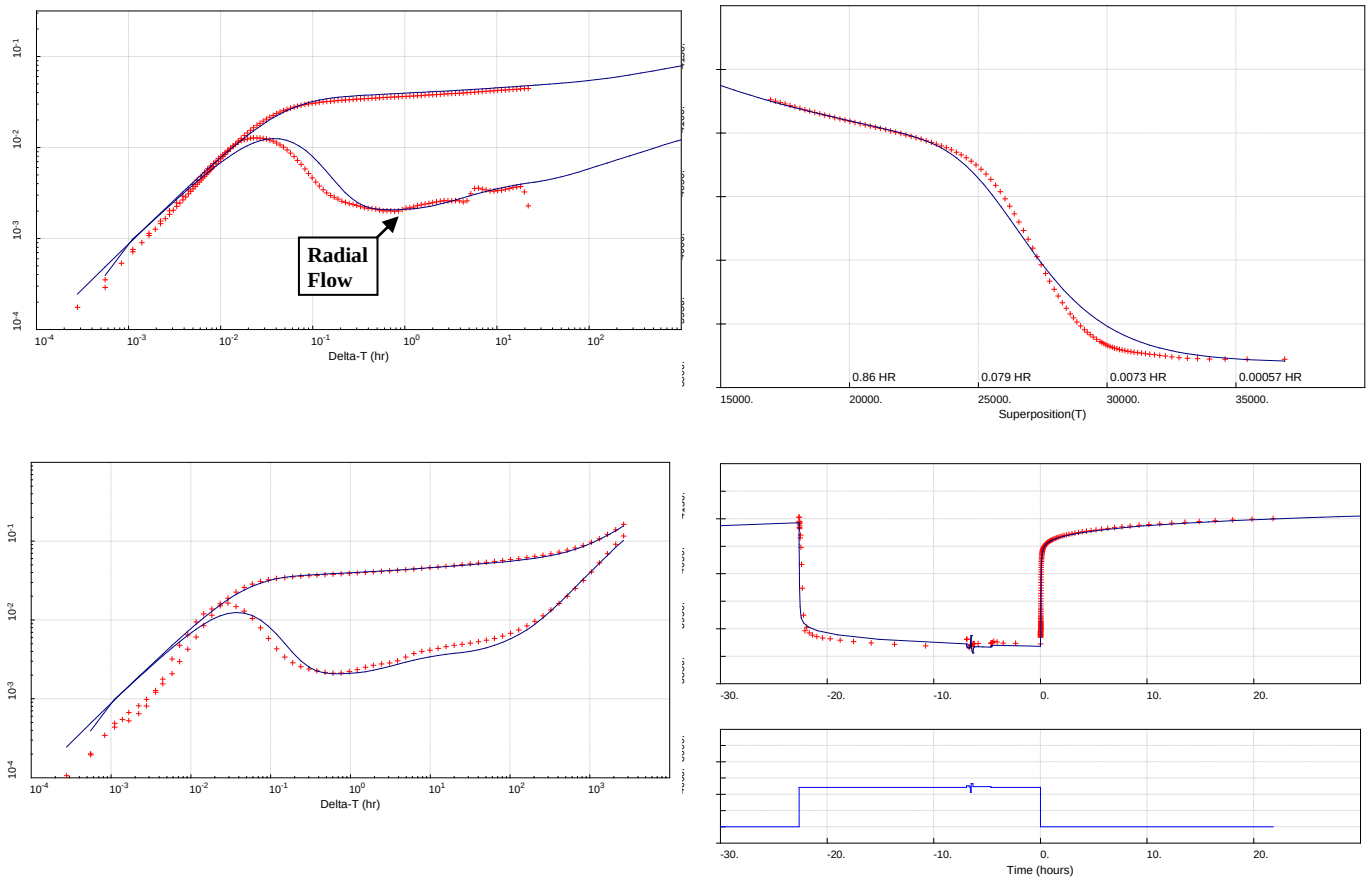

Fig. 7: Well R1 results of interpretation using, clockwise from top left: log-log and derivative analysis, superposition analysis, deconvolution and pressure history match

Well R2

Well R2 is a producer situated at the crest of the northern dome and perforated in zone B of The Sandstone. Following 6 months of production, the well was shut in for 21 hours, with a Production Logging Tool (PLT) being used to record pressures.

The well is interpreted as having a constant pressure boundary to the south due to injectors R30 and R33 as shown in Fig. 8. It is also interpreted as having limited entry, and production boundaries which intersect in the north due to producers R21 and R23. This analysis is summarised in Table 4 and Fig. 9. The following points are highlighted from the analysis:

- Interpreted permeability of 2030 is significantly higher than the c.300mD found through log interpretation
- 60% of skin appears to be Mechanical in nature
- The drainage area extends 5000ft to the south, possibly providing opportunities for production enhancement from neighbouring wells.

Table 4: Well R2 PTA interpretation

Simulation Data	partial penetration well
Well. storage	0.06 bbls/psi
Skin(mech.)	6.8
Permeability	2030
Kv/Kh	1
Eff. Thickness	195 feet
Zp/Heff	0.4
Skin(Global)	11.5
Perm-Thickness	396870. mD-feet
-y boundary	200. feet (No Flow)
Intersecting	5000. feet (Constant Pressure)
Angle	90.0 degrees
Initial Press.	3917.8 psi
Smoothing Coef	0.,0.
Deconv. Initial Press.	3917.8 psi
Conditioning Coeff.	0.01
Obj.Func.	260.1

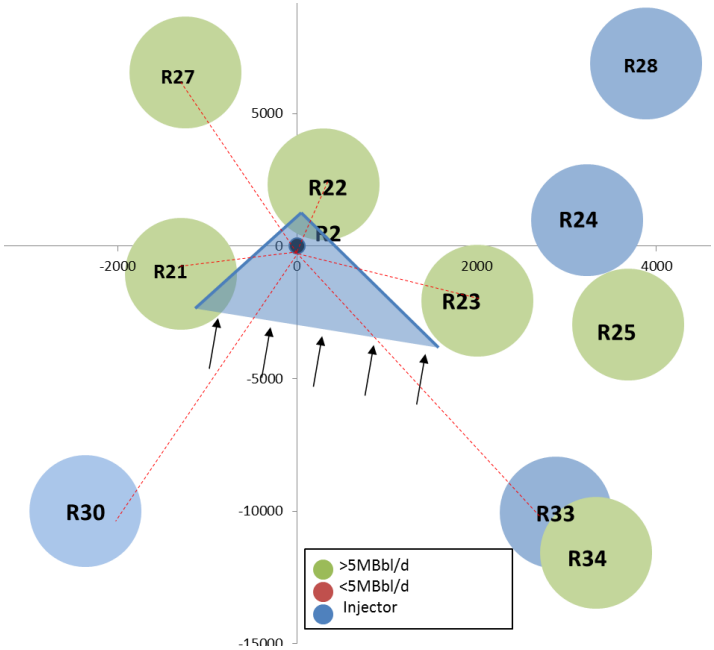

Fig. 8: Well R2 proximity to neighbouring wells, and influence on interference boundaries

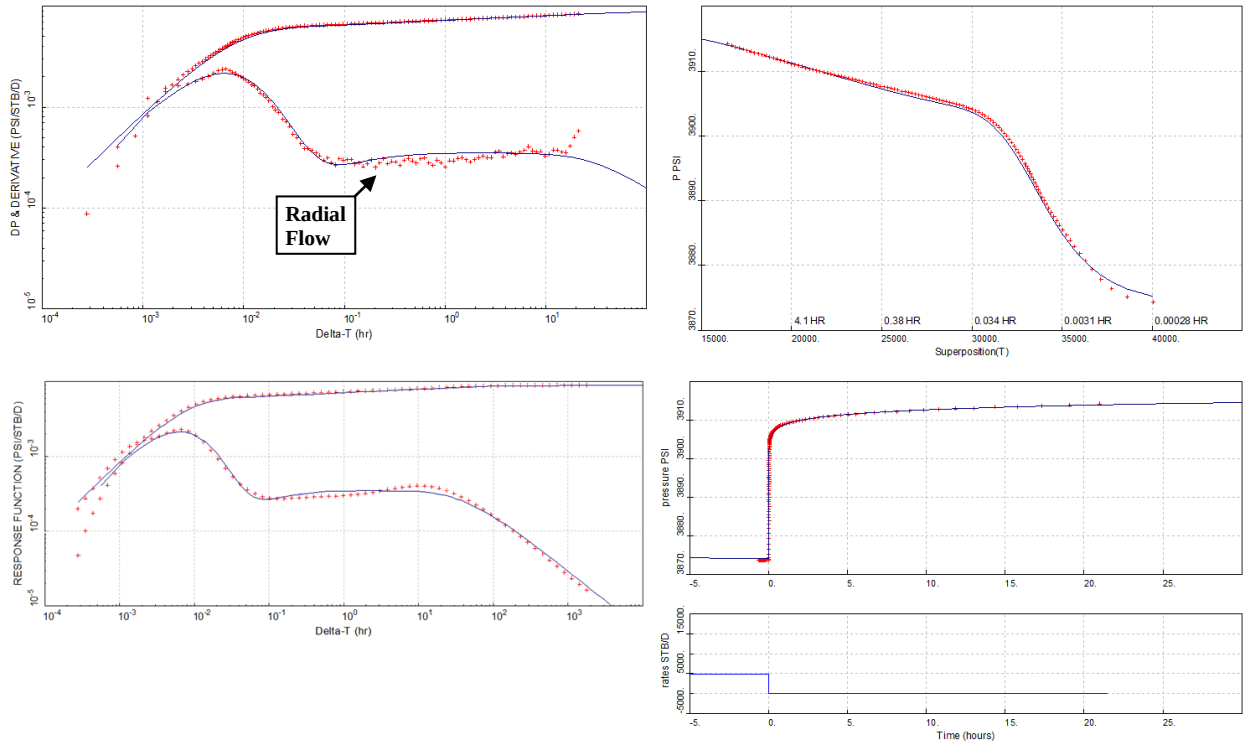

Fig. 9: Well R2 results of interpretation using, clockwise from top left: log-log and derivative analysis, superposition analysis, deconvolution and pressure history match

Well M1

Well M1 is a producer situated in the north of the northern dome, and perforated in The Limestone. Pressure transient data from this reservoir is scarce, and the age of this data results in two constraints. Firstly the sampling period of one minute in the early time makes it difficult to assess when wellbore storage ends through derivative analysis. Secondly the low pressure gauge resolution limits the analysis to 40 hours from the 65 hour build-up.

The well is interpreted as being in a closed reservoir as shown by the results of the analysis in Table 5 and Fig. 10. The geological assessment of the region shows that Well M1 lies in a localised area of high permeability carbonate, surrounded on all sides by much lower permeability rock. This interpretation is consistent with the assessment of the PTA, which shows that the change in permeability is significant enough to be seen as a barrier to flow by the well. The following points are highlighted from the analysis:

- Interpreted permeability of 172mD matches the geological interpretation of 100mD-300mD.
- Minimal skin is observed, as the PTA was conducted following an acid job.
- No-flow boundaries of 700ft-1300ft are consistent with the geological interpretation

Table 5: Well M1 PTA interpretation

Simulation Data	Homogeneous Reservoir
Well. storage	0.06 bbls/psi
Skin	1.6
Permeability	170 mD
Areal Ky/Kx	1
Perm-Thickness	59878. mD-feet
+x boundary	1050. feet (No Flow)
-x boundary	900. feet (No Flow)
+y boundary	1300. feet (No Flow)
-y boundary	750. feet (No Flow)

Initial Press.	4100 psi
Average Press.	3685 psi
Smoothing Coef	0.,0.
Deconv. Initial Press.	4101.00 psi
Model Ct	.7240e-05 1/psi
Conditioning Coeff.	0.01
Obj.Func.	9656.5

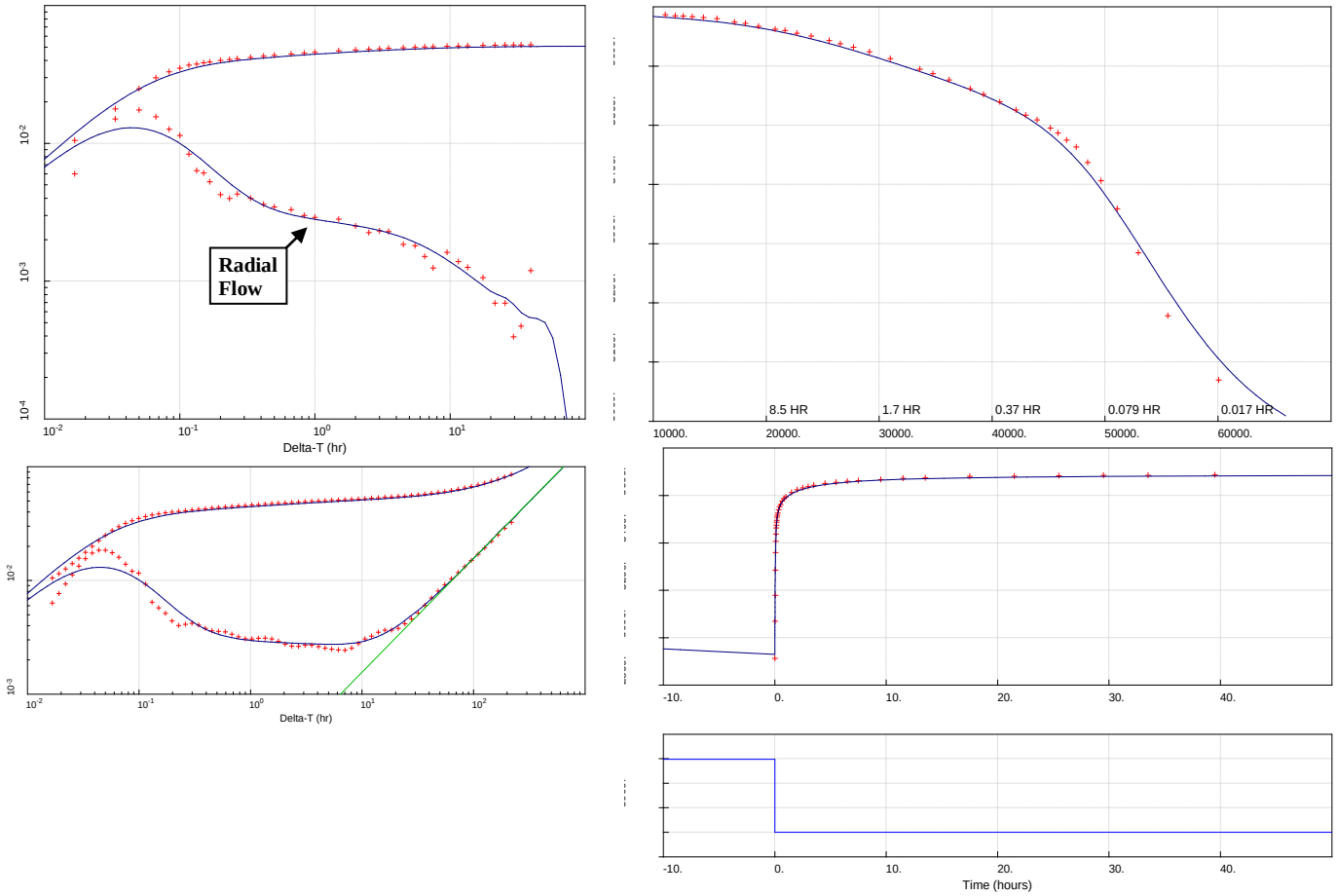

Fig. 10: Well M1 results of interpretation 1 using, clockwise from top left: log-log and derivative analysis, superposition analysis, deconvolution and pressure history match

Well M2

Well M2 is an injector situated at the crest of the northern dome, and perforated in The Limestone. When the Pressure Fall Off (PFO) commences, the wellbore is full of injection water and the bottomhole pressure is greater than the hydrostatic column $P_{HS} \approx 3600psi$ (1). As the fall off proceeds, the bottomhole pressure declines below P_{HS}, causing a "humping behaviour" to occur. This phenomenon is confirmed using a semi-log plot to show that the humping occurs at P_{HS} (Fig. 11).

$$P_{HS} = \rho g h = 0.44 * 8200psi \approx 3600 \quad \text{.....(1)}$$

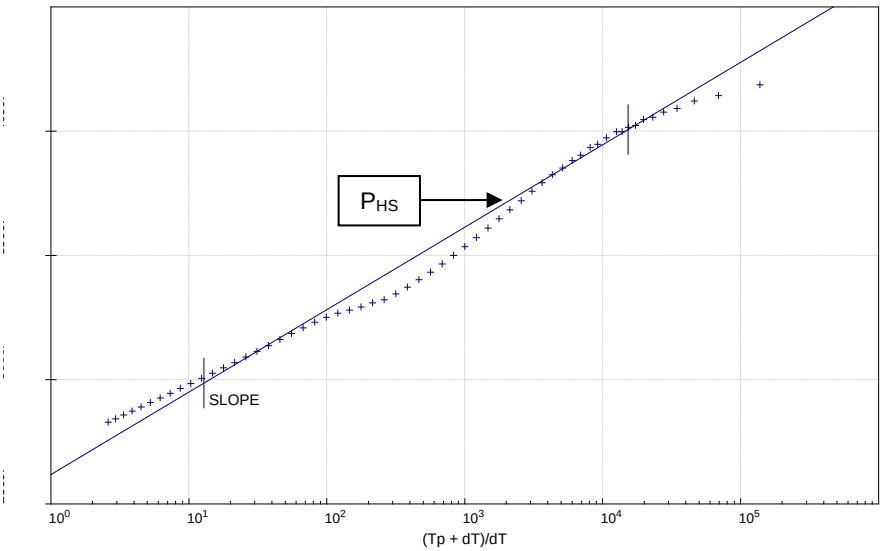

Fig. 11: Well M2 humping effect on semi-log plot, showing occurrence when pressure declines below P_{HS}

Late time behaviour is seen only through the use of deconvolution, and gives rise to an assessment of a closed reservoir. Geologically well M2 is believed to lie in a region of moderate permeability (~100mD), surrounded on all sides by very low permeability rock (0.1-10mD). This contrast in permeability appears to be sharp enough to cause no-flow boundaries leading to the closed reservoir interpretation.

The injection of water appears to have caused a region of slightly lower permeability within a radius of 20ft from the well. The reason for this is not entirely clear, but three possibilities are

a) A lower water relative permeability due to the flushing of oil in a water-wet rock
b) A lowering of temperature causing the rock contraction and inhibition to flow
c) Rock minerals reacting with the injected water causing swelling

Table 6: Well M2 PTA interpretation

Simulation Data	Radial Composite Homogeneous Reservoir
Well. storage	0.002 bbls/psi
Skin(mech.)	-2.5
Permeability	48 mD
Perm.(inner)	14.5 mD
Stor.rto+x o/i	1
Inner Radius	21 feet
Skin(Global)	-1.6
Mobility+x o/i	1.5
Perm-Thickness	6576.0 mD-feet
+x boundary	520. feet (No Flow)
-x boundary	660. feet (No Flow)
+y boundary	1200. feet (No Flow)
-y boundary	800. feet (No Flow)

Initial Press.	2805 psi
Datum Press.	2788 psi
Smoothing Coef	0.,0.
Deconv. Initial Press.	2805.1 psi
Conditioning Coeff.	0.01
Obj.Func.	103807

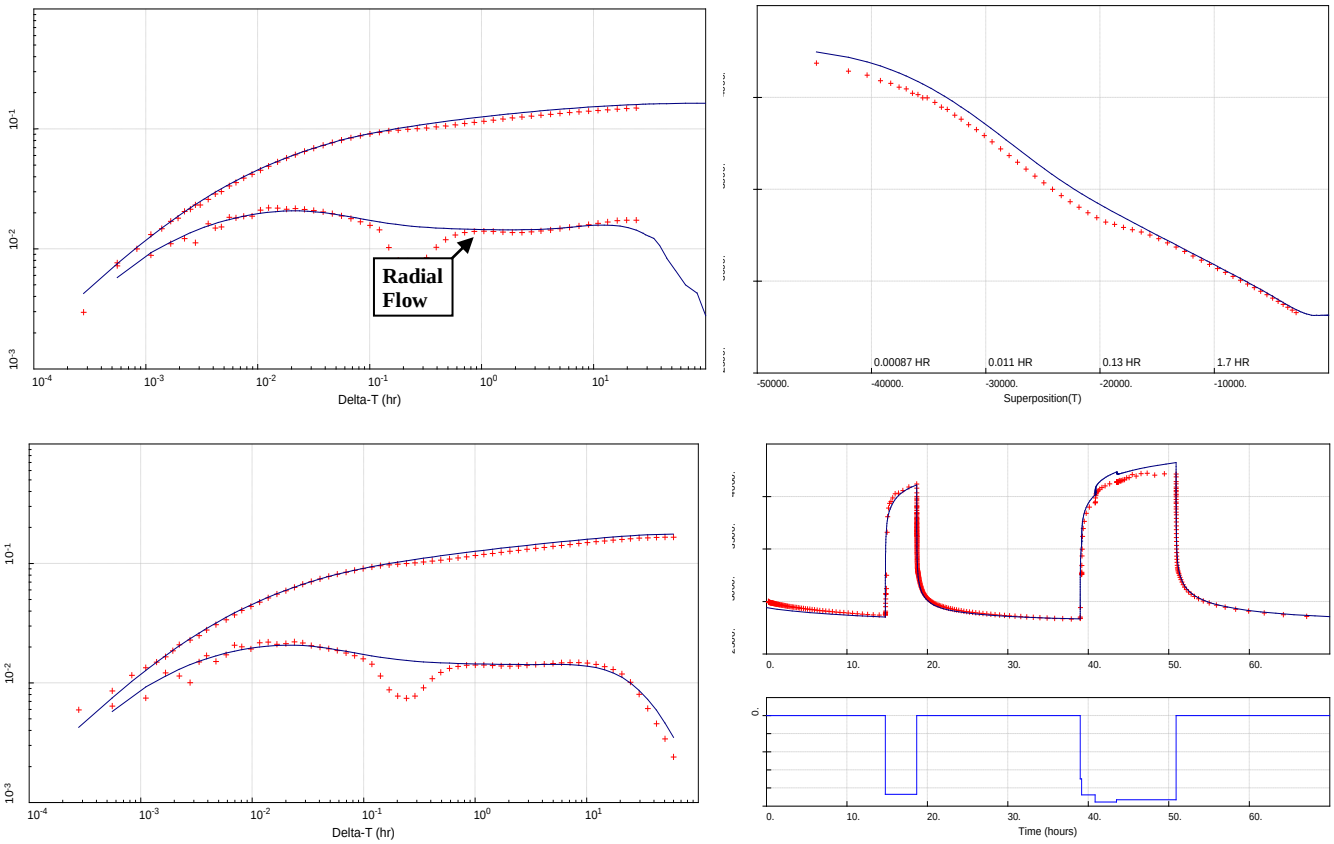

Fig. 12: Well M2 results of interpretation using, clockwise from top left: log-log and derivative analysis, superposition analysis, deconvolution and data verification

Discussion

PTA of the four wells in The Sandstone and two wells in The Limestone has been performed. This has shown that in the majority of cases the close proximity between wells leads to production boundaries which prevent late time analysis of the reservoir from taking place.

Limiting PTA to the early time allows test durations to be significantly reduced. This analysis is possible as soon as the radial flow derivative stabilisation can be identified. Table 7 summarises the time at which radial flow occurred within the six wells analysed. Based on this information, and providing for adequate contingency, an estimate of the test duration required for early time PTA to take place might be given as 3 hours.

Table 7: Summary of time until radial flow

Well	Time until Radial Flow (Hours)
U1	1
U2	0.8
R1	0.9
R2	0.2
M1	0.9
M2	0.9

Sensitivity Analysis

The time until radial flow occurs is dependent on a number of parameters, including some which can only be established through PTA. Tests exceeding the 3 hour estimate provided above may fail to reach radial flow making interpretation challenging.

The Design Application for Pressure Transient Analysis (DAPTA) has been developed as a tool for providing more comprehensive estimates of the time required for radial flow to occur. During radial flow, the dimensionless pressure can be approximated by Eq. (1). Bourdet *et al.* (1983) developed the derivative type-curve which uses the derivative group in Eq. (2) which can be shown to be equal to a value of 0.5 during radial flow. The type curve authors suggested that a 10% Approximation Percentage provides an adequate indication of radial flow. Data collected from a giant Middle Eastern oil field suggests that an Approximation Percentage of 3% is more appropriate for use in DAPTA, as this ensures a sufficient margin for error when recommending the optimum test duration.

$$P_D = \frac{1}{2}\left(ln\frac{t_D}{C_D} + 0.80907 + C_D e^{2S}\right) \quad (1)$$

$$\left(\frac{t_D}{C_D}\right)\frac{d(P_D)}{d\left(\frac{t_D}{C_D}\right)} \quad (2)$$

To assess how flow regime time limits are affected by reservoir and well properties, DAPTA was used to conduct a sensitivity analysis. Table 8 shows the static values used for the rock, fluid and well properties, as well as the ranges of wellbore storage, permeability and skin examined.

Within The Sandstone, the presence of both channel sands and shoreline sands results in a permeability range spanning almost 3 log cycles. Fig. 13 shows that this results in an equivalent range of flow regime time limits, with both time until start of radial flow, and time until end of wellbore storage spanning 3 to 4 log cycles for any given value of skin. These ranges are less considerable within The Limestone, where permeability is generally limited to between 30-300mD.

Well effects are less heterogenic than reservoir effects, with skin typically ranging from 3 to15 in most unacidised wells. The impact of this range on the flow regime time limits is less pronounced than the case of permeability. For example, this range of skin factors within a typical 1500mD rock would result in the time until wellbore storage ends ranging between 4E-3 hours and 1E-2 hours, and the time until radial flow begins ranging from one to two hours (Fig. 14).

Attempts to standardise well designs within the field, together with an inability to shut in wells downhole, significantly reduces the probable range of wellbore storage values. For almost all production wells in the field, wellbore storage lies between 0.04 and 0.08 bbl/psi. Within this range, and for all values of both skin (Fig. 15) and permeability (Fig. 16) examined, the flow regime time limits do not vary by more than a factor of 2.5. Care should be exercised especially when designing PTAs for injector wells, or those with non-standard well designs, as significant deviations from this range are likely

Table 8: Values used in sensitivity analysis

Parameter	Value	Range	Units
ϕ	19.25	/	%
μ	0.71	/	cp
c_t	1.2E-5	/	psi^{-1}
r_w	0.21	/	ft.
h_{net}	62	/	ft.
C	0.064	0.001 to 0.1	bbl/psi
k	1000	10 to 5000	mD
S	5	-3 to 30	(-)

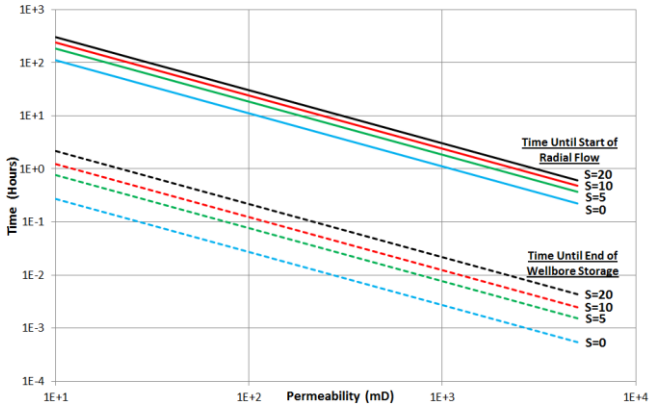

Fig. 13: Sensitivity of flow regime time limits to permeability for various values of skin

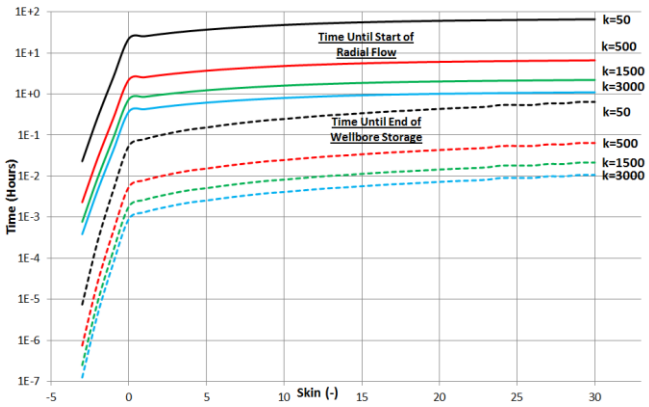

Fig. 14: Sensitivity of flow regime time limits to skin for various values of permeability

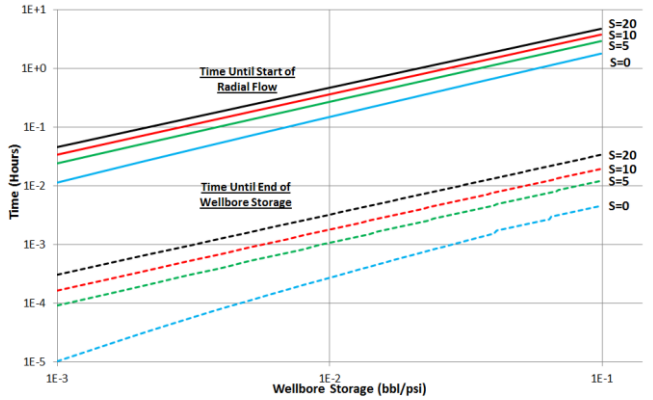

Fig. 15: Sensitivity of flow regime time limits to wellbore storage for various values of skin

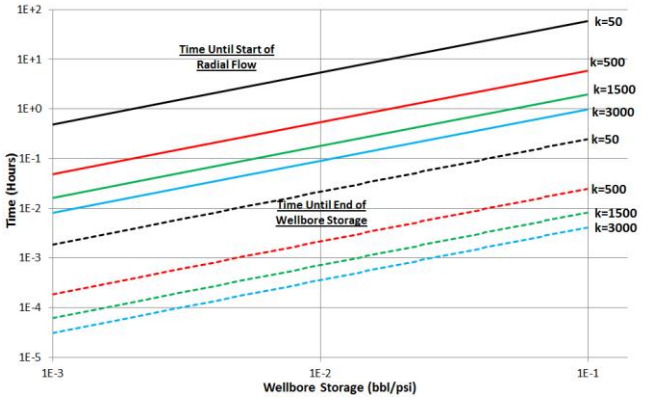

Fig. 16: Sensitivity of flow regime time limits to wellbore storage for various values of permeability

PTA of Data from ESP Gauges

Duhamel's integral (2) expresses the well pressure during variable rate production due to the principle of superposition which results from the linear nature of the system.

$$p(t) = p_0 - \int_0^t q(\tau)\frac{dp_u(t-\tau)}{dt}d\tau \quad \text{.....(2)}$$

Pressure/rate deconvolution attempts to generate the unit-rate drawdown pressure response $p_u(t)$, together with the initial reservoir pressure p_0 from pressure data p(t) and rate data q(t) collected while a well is producing at varying rates. This is achieved through a Total Least-Squares formulation which performs unconstrained nonlinear minimisation on an objective function. This objective function definition not only incorporates pressure information, but also accounts for possible errors in rate data, and constrains the curvature to achieve regularisation of an otherwise ill-conditioned problem (Von Schroeter; 2001, 2004).

Simulation Model

The model simulated was a vertical well in a homogeneous radial reservoir, closed on three sides by boundaries 1000ft away (Fig. 17). This arrangement is typical of a well in The Sandstone, with boundaries used to simulate production boundaries due to neighbouring wells.

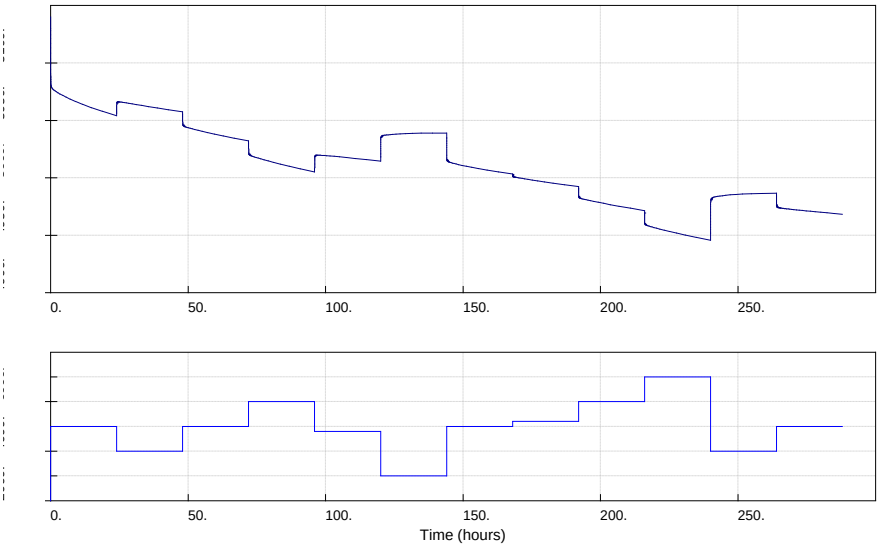

Fig. 17: Model used to simulate data from a well operating with an ESP

Parameters (Table 9) were all chosen based on typical values for a production well situated in The Sandstone. The distance between the perforations and the pressure gauge was increased to 500 feet to emulate the typical depth at which an ESP is positioned. Table 10 shows the rates used to generate the simulated data. Initially 24 hours was used for each flow period. This was replaced with 2400 hour flow periods in the final test.

Table 9: Simulated well parameters

Field	Value	Units
Oil Gravity	30	deg api
Reservoir Temperature	210	deg f
GOR	560	scf/stb
Reservoir Pressure	4022	psi
Volume Factor	1.4	-
Viscosity	0.71	cp
Oil Compressibility	1.1E-5	1/psi
Water Compressibility	3.1E-6	1/psi
Well. Storage	0.065	bbls/psi
Skin	10	(-)
Permeability	2000	mD

Field	Value	Units
Porosity	20	%
Water Saturation	10	%
Net Thickness	100	ft
Rock Compressibility	1E-6	1/psi
Wellbore Radius	0.2917	ft
Datum/Gauge Depth	10,000	ft
Top Perforation	10,500	ft
Bottom Perforation	10,600	ft
Static gradient	0.333	psi/ft
Initial Pressure	5140	psi

Table 10: Flow rates used to generate simulated data for a well with ESP

Flow Period	Rate (bpd)
1	5000
2	4000
3	5000
4	6000

Flow Period	Rate (bpd)
5	4800
6	3000
7	5000
8	5200

Flow Period	Rate (bpd)
9	6000
10	7000
11	4000
12	5000

Typical values for ESP pressure intake gauge parameters have been summarised below. These were used to ensure the simulated data reflects typical ESP pressure measurements as closely as possible. They were also used to establish suitable ranges of pressure resolution, rate error, and sampling period to be examined as part of this study.

Table A-1: Typical values and values modelled for ESP pressure intake gauge parameters

Vendor	APC	BHI
Type of pressure Gauge	Improved Strain Gauge	Strain Gauge
Resolution	0.1 psi	0.1 psi
Noise	0.1psi	0.01mA
Linear Drift	<0.1psi/hr	4.5e-4psi
Step Error	0.6psi	0.1% Full Scale
Sample Period	4s-60s	4s-60s
Rate Error	0.10%	0.10%

Value/Range Used in Model
Strain Gauge
0.1psi - 5 psi
0.1psi
0.01psi/hr
5psi
1s - 60s
0.1% - 10%

ESP Pressure Resolution

ESP pressure gauge data is typically of a relatively low resolution (0.5- 5psi). These pressures, coupled with pump frequency, and information regarding the pump rotor are used to calculate the rate. As a result, rate accuracy is directly related to pressure resolution (typically 0.1% to 10%). These uncertainties, together with variations in production rate make ESP data an ideal candidate for deconvolution.

Previous work by von Schroeter *et al.* (2002) examined errors of up to 5% in the pressure signal, and 10% in the rate signal. These authors showed that deconvolution is much more resilient to errors in rate than pressure. Levitan (2005) found that the deconvolution algorithm described could converge to the correct result even with an order of magnitude error in the rate signal. He also concluded that data must remain consistent during the flow periods deconvolved, e.g. constant wellbore storage and skin (Levitan, 2005).

To establish the minimum gauge resolution required for deconvolution to operate effectively, simulated data was used with a fixed rate error of 10%. As well as being a suitable indication of the rate error likely when using ESP data, this level of error also benefits from having been found acceptable by the studies cited above.

The work by von Schroeter *et al.* (2002) showed that combining a 10% rate error with a 0.5% pressure error caused a noticeable deviation in the deconvolved derivative, while increasing the latter to 5% would likely lead to an incorrect interpretation. Various gauge resolutions have been simulated in the present study, using a 12 day dataset with a 10% rate error (Fig. 18). With a 2psi pressure resolution the derivative is practically indistinguishable from the correct derivative. Increasing this to 5psi causes a slight deviation at the point of radial flow stabilisation, equivalent to 300mD.ft in kh. Further reducing the resolution to 8psi causes a failure of the algorithm to converge thus not generating a meaningful derivative.

The solution proposed is to increase the quantity of data in order to compensate for the lack of quality in data. This solution was validated by replacing each one day flow period with a 100 day flow period (Fig. 19). It was found that with this new data set, the derivatives for all pressure resolutions are identical to the correct derivative, and even a pressure resolution of 10psi can now be fully deconvolved.

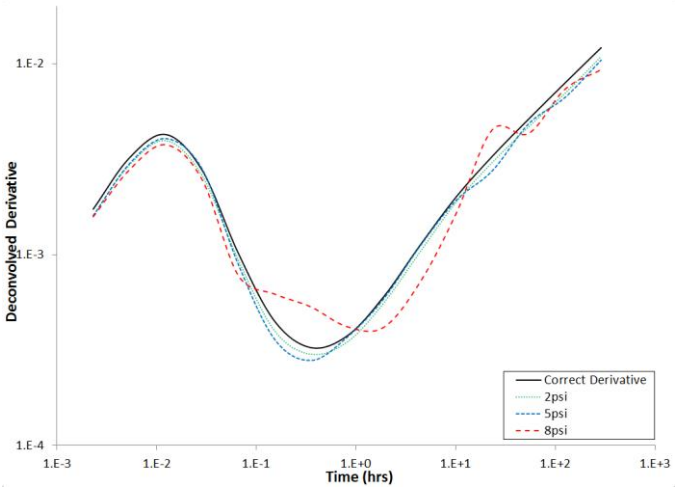

Fig. 18: Deconvolution of various pressure resolutions using 12 days of data with a 10% rate error and 1 second sampling period

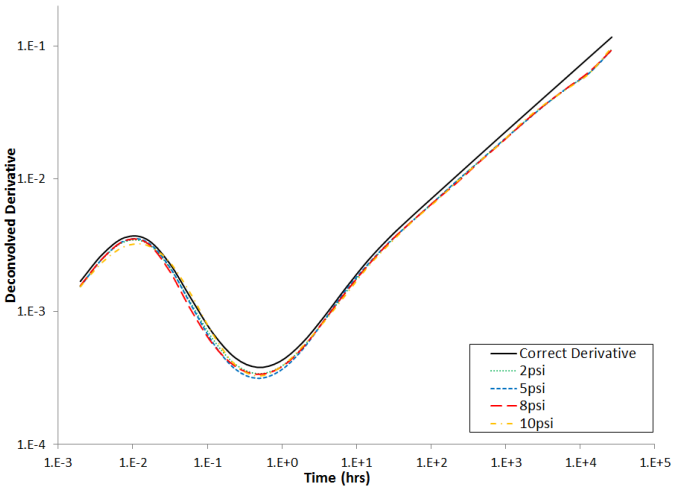

Fig. 19: Deconvolution of various pressure resolutions using 1200 days of data with a 10% rate error and 1 second sampling period

Sampling Period

Typically ESPs transmit intake pressure measurements every minute. Utilising the pressure intake mode available on many devices reduces this to four seconds. Unfortunately the increase in data transmission from the ESP comes at the expense of other parameters, such as temperature, which may be crucial for the efficient operation of the ESP. For this reason, pressure intake mode is rarely implemented for extended durations.

To assess how reduced data sampling frequencies impact deconvolution, the 12 day dataset was again utilised with a 10% rate error. For pressure resolutions of 1psi, there is sufficient data available such that even with an entire minute between pressure measurements the deconvolved derivative is indistinguishable from the correct derivative. With the case of 2psi (Fig. 20), a 60 second sampling period now causes a slight deviation from the correct behaviour, but this would not affect any interpretation. With a 5psi resolution, the data limit of deconvolution is clearly illustrated by a gradual collapse of early time behaviour, corresponding to the deconvolution algorithm being gradually provided less data. In all cases, the late time behaviour is indistinguishable from the correct derivative.

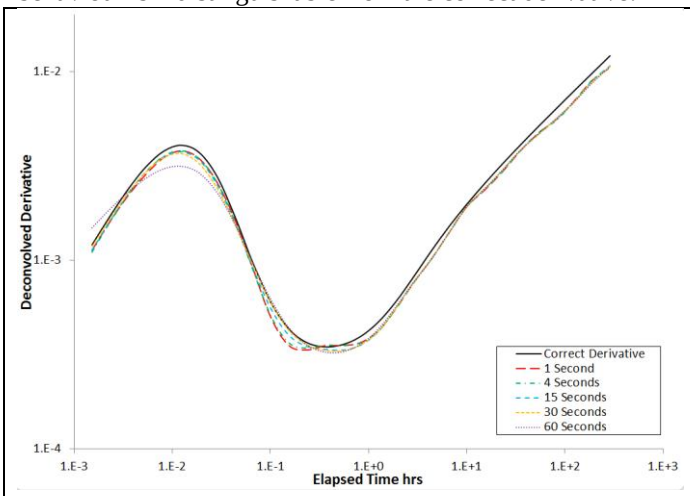

Fig. 20: Deconvolution of various sampling periods using 12 days of data with a 10% rate error and 2 psi pressure gauge resolution

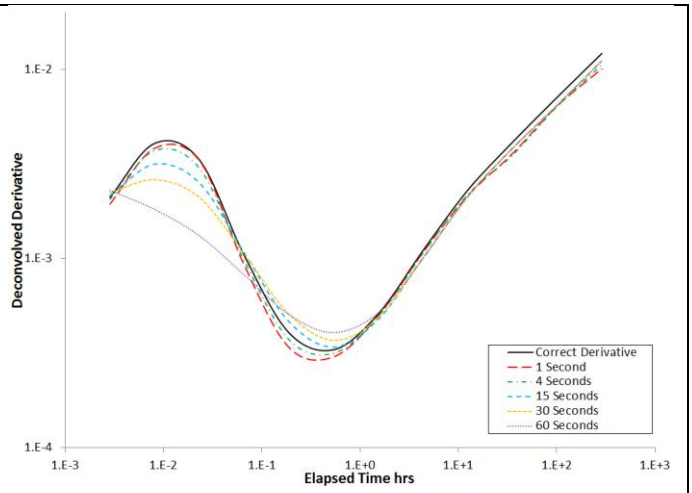

Fig. 21: Deconvolution of various sampling periods using 12 days of data with a 10% rate error and 5 psi pressure gauge resolution

Conclusions

Pressure Transient Analysis (PTA) of six wells from a giant Middle Eastern field has shown that there is limited value in performing late time PTA in that field. An estimate of the test duration required for early time PTA to yield kh and skin effect has been found to be approximately 3 hours. A sensitivity analysis showed that this duration is highly dependent on formation permeability which varies considerably due to reservoir heterogeneities, especially in The Limestone reservoir.

Performing deconvolution on pressure and rate data collected from Electrical Submersible Pump gauges allows pressure transient analysis to be conducted without shutting in a well. Main results from analytical simulations are:

- Pressure/rate deconvolution is possible, even with very low quality data (10psi resolution), provided data quality is compensated with data quantity;
- The deconvolved derivative generated using a pressure resolution of 2psi, a sampling period of 60 seconds, and a rate error of 10% is practically indistinguishable from the correct derivative;

Recommendations for Further Study

1. Examine the effect of high water-cut on performing PTA of ESP gauge data, as ESPs are typically installed on wells which are unable to flow naturally due to high water-cut.
2. Attempt to conduct PTA of real data collected from ESP gauges, as this study has only examined simulated ESP gauge data.

Acknowledgements

The author would like to thank the field operating organisation for providing data for use within this study.

Nomenclature

B	Formation volume factor (rb/stb)	q	Flow rate (stb/d)
c_{well}	Well fluid compressibility (1/psi)	q_A	Fluid unloaded from annulus (bbl/s)
c_t	Formation total compressibility (1/psi)	r_{inv}	Radius of investigation (ft)
C	Wellbore storage constant (bbl/psi)	r_w	Wellbore radius (ft)
C_D	Dimensionless wellbore storage constant (-)	s	Laplace domain variable
C_{FE}	Fluid expansion wellbore storage constant (ft^3/psi)	S	Skin (-)
C_{LL}	Liquid loading wellbore storage constant (ft^3/psi)	S_w	Water Saturation (fraction)
g	Acceleration of gravity (ft/s^2)	t	Time (various)
g_c	Units conversion factor = 32.17 (lb_m ft/lb_f s^2)	t_D	Dimensionless time (-)
h	Formation net thickness (ft)	V_u	Wellbore volume per unit length (ft^3/ft)
k	Permeability (mD)	$V_i(N)$	Array of inverse Laplace estimation constants for N iterations
L	Wellbore depth (ft)	V_{well}	Total wellbore volume (bbl)
L_1	Depth to packer (ft)	x'_D	Dimensionless parameter x using effective wellbore radius
p	Pressure (psi)	Δx	Change in parameter x (various)
p_0	Initial reservoir pressure (psi)	μ	Viscosity (cp)
p_D	Dimensionless pressure (-)	ρ	Density (lb_m/ft^3)
p_u	Unit-rate drawdown pressure response (psi/[stb/d])	ϕ	Porosity (fraction)

$L\{x\}$	Laplace domain function x
K_0	Modified Bessel function, second kind, zero order
K_1	Modified Bessel function, second kind, first order
Fa(L{x})	Approximate inversion of Laplace domain function x

Table 11: Table of units used in this study, and conversion factors implemented within DAPTA

Parameter	Units		DAPTA Conversion Factors
Distance	ft	feet	
Distance	m	meters	1m = 0.305ft
Distance	in	inches	1inch = 0.083ft
Time	h	hours	
Time	d	days	1day = 24 hours
Time	s	Seconds	1second = 2.78E-4 hours
Pressure	psi	$lb_f\ per\ inch^2$	
Density	API^o	Degrees API	$\rho\ (lb_m/ft^3) = \left(\frac{141.5}{API^o + 131.5}\right) * 62.43$
Mass	lb_m	Pounds mass	
Force	lb_f	Pounds force	
Various	$-$	Dimensionless parameter	
Permeability	mD	milliDarcy	
Volume	rb	Reservoir barrels	
Volume	stb	Stock tank barrels	
Viscosity	cp	centipoise	

References

Agarwal, R. G., Al-Hussainy, R., and Ramey H.J.: "An Investigation of Wellbore Storage and Skin Effect in Unsteady Liquid Flow: I. Analytical Treatment," *SPE Journal* (Sept. 1970) **10,** No. 3, 279-290.

Bourdet, D.P., and Gringarten, A.C.: "Determination of Fissure and Block Size in Fractured Reservoirs by Type-Curve Analysis," paper SPE 9293 presented at the 1980 SPE Annual Technical Conference and Exhibition, Dallas, 21 -24 Sept.

Bourdet, D., Whittle, T.M., Douglas, A.A., Pirard, Y.M.: "A new set of type curves simplifies well test analysis", World Oil (May 1983) 95-106.

Gaver, D.P. Jr.: "Observing Stochastic Processes and Approximate Transform Inversion," *Operations Research* (1966) **14**, No. 3, 444-459

Gringarten, A.C., Bourdet, D.P., Landel, P.A. and Kniazeff, V.J.: "A Comparison between Different Skin and Wellbore Storage Type-Curves for Early-Time Transient Analysis," paper SPE 8205 presented at the 1979 Annual Technical Conference and Exhibition, Las Vegas, 23 -26 Sept.

Levitan, M.M.: "Practical Application of Pressure-Rate Deconvolution to Analysis of Real Well Tests," SPEREE (2005) **8**, No. 2, 113-121.

Levitan, M.M., Crawford, G.E., and Hardwick, A.: "Practical Considerations for Pressure-Rate Deconvolution of Well-Test Data," *SPE Journal* (Mar. 2006) **11**, No. 1, 35-47.

Ramey, H.J. Jr.: "Non-Darcy Flow and Wellbore Storage Effects in Pressure Build-Up and Drawdown of Gas Wells," *Journal of Petroleum Technology* (Feb. 1965) **17**, No. 2, 223-233.

Stehfest, H.: "Numerical Inversion of Laplace Transforms," *Communications of the ACM* (Jan. 1970) **13**, No.1, 47-48. (Algorithm 368 with correction (October 1970) 13, No. 10).

van Everdingen, A.F. and Hurst, W.: "The Application of the Laplace Transformation to Flow Problems in Reservoirs," *Journal of Petroleum Technology* (Dec. 1949) **1**, No. 12, 305-324.

van Poollen, H.K.: "Radius-of-Drainage and Stabilization Time Equations," *Oil and Gas Journal* (Sept. 1964) **62**, No. 1, 138-146.

von Schroeter, T., Hollaender, F., and Gringarten, A.C.: "Deconvolution of Well Test Data as a Nonlinear Total Least Squares Problem," paper SPE 71574 presented at the 2001 SPE Annual Technical Conference and Exhibition, New Orleans, 30 Sept. – 3 Oct.

von Schroeter, T., Hollaender, F., and Gringarten, A.C.: "Analysis of Well Test Data From Permanent Downhole Gauges by Deconvolution," paper SPE 77688 presented at the 2002 SPE Annual Technical Conference and Exhibition, San Antonio, 29 Sept – 2 Oct.

von Schroeter, T., Hollaender, F., and Gringarten, A.C.: "Deconvolution of Well Test Data as a Nonlinear Total Least Squares Problem," *SPE Journal* (Dec. 2004) **9,** No. 4, 375-390.

Appendix A: Literature Review

Table A-1: Key milestones related to this study

SPE Paper n°	Year	Title	Authors	Contribution
2336-PA	1970	"Short-Time Well Test Data Interpretation in the Presence of Skin Effect and Wellbore Storage"	Ramey Jr., H.J	First to suggest the use of log/log type curves as an effective tool for Well Test Analysis.
8205-MS	1979	"A comparison between different skin and wellbore storage type-curves for early-time transient analysis"	Alain C. Gringarten, Dominique P. Bourdet, Pierre A. Landel, Vladimir J. Kniazeff	First to introduce the concept of independent variables to type curve analysis. First to provide an integrated Well Test Analysis methodology.
World Oil	1983	"A new set of type curves simplifies Well Test Analysis"	Bourdet, D.P., Whittle, T.M., Douglas, A.A, Pirad, Y.M.	First to suggest the use of derivative type curves for disseminating information from a Well Test Analysis.
71574-MS	2001	"Deconvolution of Well Test Data as a Nonlinear Total Least Squares Problem"	Thomas von Schroeter, Florian Hollaender, Alain C. Gringarten	First to suggest a deconvolution technique which uses nonlinear Total Least Squares to account for measurement uncertainties.
77688-MS	2002	"Analysis of Well Test Data From Permanent Downhole Gauges by Deconvolution"	Thomas von Schroeter, Florian Hollaender, Alain C. Gringarten	First to recommend against estimation of initial pressure in the deconvolution process
84290-MS 84290-PA	2003 2005	"Practical Application of Pressure/Rate Deconvolution to Analysis of Real Well Tests"	Michael M. Levitan,	First to provide a critical evaluation of von Schroeter et al. deconvolution algorithm. First to identify that said algorithm fails when subjected to inconsistent data, and to suggest enhancements allowing it to be used reliably in such cases.
90680-PA	2006	"Practical Considerations for Pressure-Rate Deconvolution of Well-Test Data"	Michael M. Levitan, Gary E. Crawford, Andrew Hardwick	First to suggest that accurate reconstruction of constant rate drawdown system response is possible even with a simplified rate history, and to specify the conditions under which this can occur.

SPE 2336 (1970)

Short-Time Well Test Data Interpretation in the Presence of Skin Effect and Wellbore Storage

Authors: Ramey Jr., H.J

Contribution to the understanding of Well Test Analysis:
Introduced the use of log/log type curves, revolutionising Well Test Analysis.

Objective of the paper:
To demonstrate a practical methodology for interpreting short-time well test data, and thus assessing wellbore storage, well damage (skin) and well fracturing.

Methodology used:
Using the usual definitions for dimensionless time (t_D), pressure (p_D) and storage constant ($\bar{C}$); and the van Everdingen-Hurst dimensionless skin factor (s):

$$t_D = \frac{0.000264kt}{\phi\mu c_t r_{10}^2}; \quad p_D = \frac{kh(p_i - p_{wf})}{141.2q\mu B}; \quad \bar{C} = \frac{C}{2\pi h\phi c_t r_{10}^2}; \quad s = \frac{kh(\Delta p_{skin})}{141.2q\mu B}$$

The logarithm of t_D and p_D where taken yielding:

$$\log t_D = \log\left(\frac{0.000264k}{\phi\mu c_t r_{10}^2}\right) + \log(t); \text{ and } \log p_D = \log\left(\frac{kh}{141.2q\mu B}\right) + \log(p_i - p_{wf})$$

It was thus shown that the only difference between a log-log plot of p_D versus t_D, and Δp versus time was a shift of both coordinates by constant amount. It was suggested that type-curve matching can then by utilised to determine the value of these constants.

Conclusion reached:

- Analysis using log-log type-curves allows substantially more to be discovered about a well than was possible from traditional build-up plots. The significance of wellbore storage is usually evident on the type-curve if sufficient information is recorded directly after shut-in.
- A significant amount can be learned from the early data recorded prior to the emergence of a straight line on a traditional plot.

Comments:
None

SPE 8205 (1979)

A comparison between different skin and wellbore storage type-curves for early-time transient analysis

Authors: Alain C. Gringarten, Dominique P. Bourdet, Pierre A. Landel, Vladimir J. Kniazeff

Contribution to the understanding of Well Test Analysis:
Introduced the concept of independent variables to type curve analysis. Integrated previous techniques into a single Well Test Analysis methodology.

Objective of the paper:
- To examine the relationship between conventional and modern interpretation techniques.
- To introduce a new, more efficient, type curve for wells with wellbore storage and skin

Methodology used:
The new type-curve is introduced as P_D versus t_D/C_D, with each substituent curve being characterised a value of C_De^{2s}; where all dimensionless parameters have their usual definitions:

$$t_D = \frac{0.000264kt}{\phi\mu c_t r_w^2}; \quad p_D = \frac{kh\Delta p}{141.2q\mu B}; \quad C_D = \frac{0.8936C}{\phi c_t h r_w^2}; \quad s = \frac{kh(\Delta p_{skin})}{141.2q\mu B}$$

The type curve is used in the usual manner; by plotting the test data Δp against Δt on log/log scales and matching against one of the curves.

Conclusion reached:
The new type-curve is applicable to both fractured and non-fractured wells. It covers a much wider array of well-conditions than previously published type-curves, and is hence deemed more efficient as an interpretation tool when wellbore storage remains constant

Comments:
None

World Oil (1983)

An Investigation of Wellbore Storage and Skin Effect in Unsteady Liquid Flow: I. Analytical Treatment

Authors: Bourdet, D.P., Whittle, T.M., Douglas, A.A, Pirad, Y.M.

Contribution to the understanding of Well Test Analysis:
First to suggest the use of derivative type curves for disseminating information from a Well Test Analysis.

Objective of the paper:
To present type-curves which greatly simplify the evaluation of buildup well test information.

Methodology used:
The authors differentiated the two dominating flow regimes. This showed that for wellbore storage:

$$\frac{d(p_D)}{d(t_D/C_D)} = p'_D = 1$$

While for radial flow:

$$\frac{d(p_D)}{d\left(\frac{t_D}{C_D}\right)} = p'_D = \frac{0.5}{t_D/C_D}$$

Thus the conclusion was reached that producing a derivative type curve would allow these flow regimes to be easily identified.

Conclusion reached:
- Interpretation is performed using a single plot of pressure that combines the benefits of both type-curve matching and semi-log analysis
- The match-point is fixed without ambiguity
- Due to the shape sensitivity of the type curves to changes in C_De^2, the match curve is also fixed

Comments:
None

SPE 71574 (2001)

Deconvolution of Well Test Data as a Nonlinear Total Least Squares Problem

Authors: Thomas von Schroeter, Florian Hollaender, Alain C. Gringarten

Contribution to the understanding of Deconvolution:
After several attempts by various authors, this paper succeeded in publishing a deconvolution algorithm which is robust enough to function with noisy pressure and rate data which are present in real well data.

Objective of the paper:
- Provide an overview of algorithms which have been suggested over the previous 40 years for the deconvolution of pressure and flow rate data.
- Suggest a new algorithm based on the logarithm of the response function.
- Introduce a new error model which accounts for errors in both pressure and rate data.

Methodology used:
The new algorithm encodes the solution using a logarithm function such that sign constraints become unnecessary. Taking the relationship between pressure drop and reservoir response:

$$tg(t) = \frac{d\Delta p(t)}{d\ ln\ t} \quad \ldots\ldots (1)$$

The solution to the superposition principal is found by taking the log so that:

$$z(\sigma) = ln\{tg(t)\}, \qquad \sigma = ln\, t, \qquad t \in [0, T] \quad \ldots\ldots (2)$$

The superposition then becomes:

$$\Delta p(t) = \int_{-\infty}^{ln\, T} e^{z(\sigma)} q(t - e^{\sigma}) d\sigma \quad \ldots\ldots (3)$$

The errors introduced due to rate uncertainties are overcome by formulating the problem as one of Total Least Squares. The problem is structured as one of unconstrained nonlinear minimisation with the residuals from (3), any rate errors, and any curvature constraints, all being included within the defined objective function.

Conclusion reached:
- Previous attempts at deconvolution of pressure and flow rate data fail to produce interpretable results with errors of 5% in pressure signal and 1% in rate signal yielding them unusable for practical purposes.
- A new method is proposed which structures the problem as one of Total Least Squares. This method has been found to successfully deconvolve simulated data with errors of 10% in the rate data.

Comments:
It is suggested that an estimate of initial pressure based on the trend of the measured rates is sufficient, and that the method is not dependent on initial pressure.

SPE 77688 (2002)

Analysis of Well Test Data From Permanent Downhole Gauges by Deconvolution

Authors: Thomas von Schroeter, Florian Hollaender, Alain C. Gringarten

Contribution to the understanding of Deconvolution:
Provides minor modifications to the algorithm proposed by von Schroeter *et al.* (2001). Recommends against estimating average initial pressure in the deconvolution process if both rates and response are unknown.

Objective of the paper:
- To provide minor modifications to the algorithm proposed by von Schroeter *et al.* (2001), and a list of unresolved issues.
- To derive analytic expressions for the expected bias vector and the covariance matrix of the estimated parameter set based on simple Gaussian models for the measurement errors in pressure and rate signals.
- To provide results from some larger field examples, including one which allows direct comparison with derivative analysis.

Methodology used:
- Used a variant of the original von Schroeter algorithm with a subtle change which allows estimates for bias and confidence intervals or the parameters
- Tested the algorithm using
  - One sets of simulated data, with 5 different combinations of error levels
  - Two sets of real test data from large fields

Conclusion reached:
Within reasonable limits of data quality, and provided a careful choice of process parameters, the method produces reliable estimates.

Comments:
Contrary to von Schroeter *et al.* (2001), this paper recommends against estimating average initial pressure in the deconvolution process if both rates and response are unknown.

SPE 84290 (2005)

Practical Application of Pressure/Rate Deconvolution to Analysis of Real Well Tests

Authors: Michael M. Levitan

Contribution to the understanding of Deconvolution:
Identified that the algorithm suggested by von Schroeter *et al.* (2001.) fails when used with inconsistent data, such as wellbore storage or skin varying during well-test. Describes enhancements to this algorithm to overcome this constraint.

Objective of the paper:
To evaluate performance and identify possible limitations of the deconvolution algorithm suggested by von Schroeter *et al.* (2001).

Methodology used:
- Used a variant of the von Schroeter algorithm with a number of subtle differences
- Used the algorithm for unconstrained minimization by Dennis and Schnabel instead of the variable projection algorithm suggested in the von Schroeter algorithm.
- Modified the definition of the objective function for least squares minimisation and the minimisation parameters
- Validated the algorithm using
  - Two sets of simulated data
  - Three sets of real test data

Conclusion reached:
- The von Schroeter algorithm works well on consistent test data, but fails when use with inconsistent data such as is found in most real test data.
- This challenge is overcome if the algorithm is slightly modified such that is can be used with the pressure data from an individual flow period. Deconvolution can then be performed one flow period at a time. The results from multiple deconvolutions can then be evaluated and contrasted.
- When applied to real test data, the von Schroeter algorithm used in the way suggested allows additional insights into pressure-transient behaviour and extracts more information than conventional well-test analysis techniques.

Comments:
Data fitting is performed only on the response-function parameters for a given value of initial reservoir pressure and for given rate data. It is suggested that to make a judgment regarding the validity of these parameters requires comparison of the deconvolved responses obtained by separate deconvolutions of pressure data from several build-ups.

SPE 90680 (2006)

Practical Considerations for Pressure-Rate Deconvolution of Well-Test Data

Authors: Michael M. Levitan, Gary E. Crawford, Andrew Hardwick

Contribution to the understanding of Deconvolution:
Suggested that accurate reconstruction of constant rate drawdown system response is possible even with a simplified rate history, and specified the conditions under which this can occur.

Objective of the paper:
To identify and discuss a number of specific issues which are important when using deconvolution. To provide practical considerations and recommendations on how to produce correct deconvolution results.

Methodology used:
Used the deconvolution algorithm suggested by von Schroeter *et al.* (2001) with the variations suggested by Levitan (2005). Emphasised four key considerations while using the approach:
The superposition principle behind deconvolution is valid only for linear systems. Maintaining single phase flow throughout the entire test sequence is therefore recommended.
The deconvolution algorithm assumes pressure is uniform throughout the reservoir when production begins. Well rate data should account for all production from this initial equilibrium state.
There must be an accurate estimate of initial reservoir pressure. It may be possible to verify or refine this estimate if multiple build-ups exist.
Deconvolution should be applied only to the portions of test pressure data that are of adequate quality.
This approach was applied to three real test examples.

Conclusion reached:
- When using deconvolution, it is good practice to use a detailed and accurate representation of the well rate history. However deconvolution can also be achieved with a simplified rate history provided:
- The time span of the rate data is preserved
- Well rate honours cumulative well production
- Well rate data accurately represent the major details of the true rate history for a period immediately before the start of the build-up. This period should be twice the length of the build-up, and rate history prior to this period may be averaged.

Comments:
As discussed by Levitan (2005), this paper emphasises that initial reservoir pressure cannot be established from a single build-up period. The paper also highlights that deconvolution of a single build-up is very sensitive to initial reservoir pressure, affecting the pressure response at late time.

Appendix B: Well U1 Data Quality Check and Static Data

Well U1 was subject to flow performance tests totalling 20.76 hours. Following this, the well was shut in for 39 hours. Two memory gauges were used and include the final drawdown and the buildup. Gauge 2, having been more recently calibrated was used in the PTA. A short drawdown occurred at the end of wellbore storage flow due to operational challenges. The duration of this drawdown is believed to be short enough not to affect the derivative analysis. As a precaution, the deconvolved derivative was also analysed as it precludes any such effects. The pressure data showed some noise during the late time. A derivative smoothing factor of 3% was to counter this (Fig. B-1)

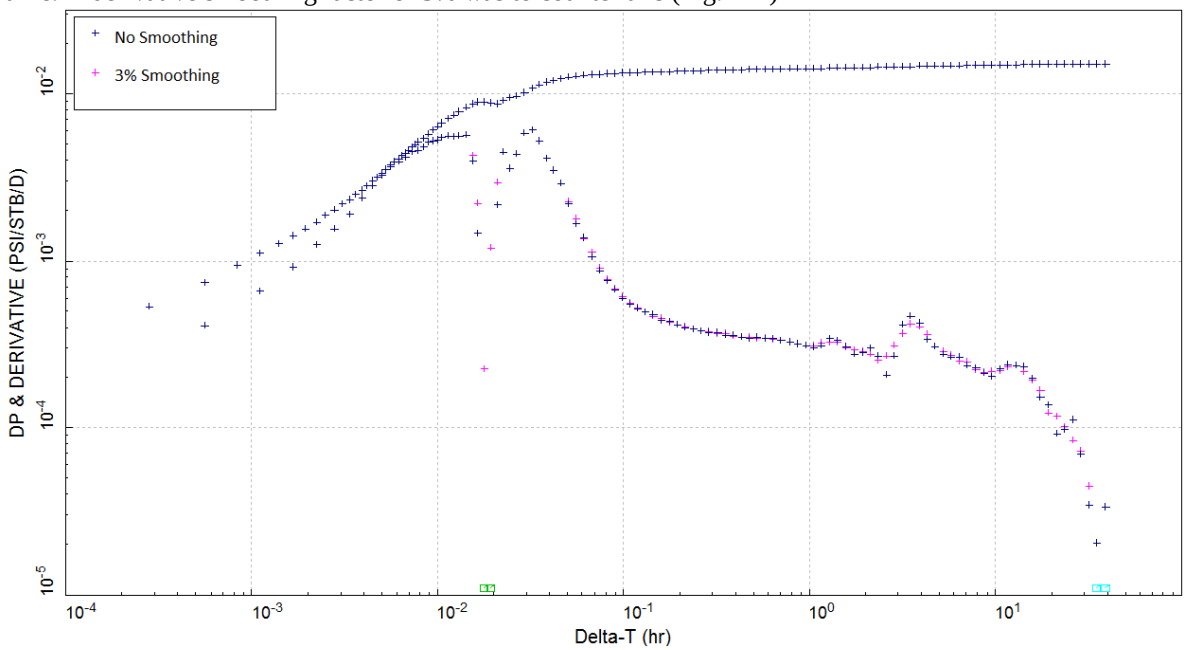

Fig. B-1: Well U1 derivative curve effects of applying a 3% smoothing factor

Rate data from the flow test was used where available. The test package was bypassed overnight with the well flowing directly to the production pipeline, preventing rate readings from being captured. During this period, the final rate from the previous flow period was extrapolated through the night. Back allocated daily production rates exist from the date the well began production, and these were used to complete the production history prior to the start of flow testing.

Table B-1: Well U1 fluid data

Field	Value	Units	Source
Oil Gravity	30	deg api	Well testing report
GOR	560	scf/stb	Well testing report
Volume Factor	1.4	-	Depletion plan
Viscosity	0.71	cp	PVT analysis
Oil Compressibility	1.13E-5	1/psi	Reservoir simulation model
Water Compressibility	3.1E-6	1/psi	Reservoir simulation model

Table B-2: Well U1 reservoir and well data

Field	Value	Units	Source
Porosity	19.25	%	Petrophysical logs
Water Saturation	6.77	%	Petrophysical logs
Net Thickness	131.7	ft	Petrophysical logs
Rock Compressibility	1E-6	1/psi	Typical Values
Wellbore Radius	0.2917	ft	Completion report
Perforated thickness	62.4	ft	Completion report + petrophysics logs. Perforated interval x Net to Gross for zone.
Reservoir Temperature	210	deg f	Well testing downhole gauge measurement
Reservoir Pressure	4022	psi	Well testing downhole gauge measurement at end of shut in

Appendix C: Well U2 Data Quality Check and Static Data

Well U2 was subject to flow performance tests over a period of 96 hours between. Following this, the well was shut-in for 27.83 hours. Two memory gauges were used and include the final drawdown and the build-up. Gauge 1, having been more recently calibrated was used in the PTA. Rate data from the flow test was used where available. The test package was bypassed overnight with the well flowing directly to the production pipeline, preventing rate readings from being captured. Back allocated daily production rates exist from the date the well began production, and these were used to complete the production history prior to the start of flow testing.

Table C-1: Well U2 fluid data

Field	Value	Units	Source
Oil Gravity	32.6	deg api	Well testing report
GOR	500	scf/stb	Well testing report
Volume Factor	1.4	-	Depletion plan
Viscosity	0.71	cp	PVT analysis
Oil Compressibility	1.13E-5	1/psi	Reservoir simulation model
Water Compressibility	3.1E-6	1/psi	Reservoir simulation model

Table C-2: Well U2 reservoir and well data

Field	Value	Units	Source
Porosity	20	%	Petrophysical logs
Water Saturation	10	%	Petrophysical logs
Net Thickness	21.3 + 177.1= 198.4	ft	Petrophysical logs
Rock Compressibility	1E-6	1/psi	Typical Values
Wellbore Radius	0.2917	ft	Completion report
Perforated thickness	26.6 + 80.7 = 107.3	ft	Completion report + petrophysics logs. Perforated interval x Net to Gross for zone.
Reservoir Temperature	205	deg f	Well testing downhole gauge measurement
Reservoir Pressure	3840	psi	Well testing downhole gauge measurement at end of shut in

Appendix D: Well R1 Data Quality Check and Static Data

Well R1 was subject to flow performance tests over a period of 172 hours. During this period the well was shut in twice. The first shut-in lasted 31.67 hours and was initiated due to a lack of space for oil in the de-gassing station. Since the memory gauges had not yet reached reservoir depth, pressures were not recorded for this build-up. The second shut-in lasted 21.85 hours. Two memory gauges were used and include the drawdown which separates the two build-ups, and the second build-up. Gauge 1, having been more recently calibrated was used in the PTA.

Rate data from the flow test was used where available. The test package was bypassed overnight with the well flowing directly to the production pipeline, preventing rate readings from being captured. The test package was also bypassed during all testing which occurred on 13 March 2012, with the following comment being recorded "Flowing the well on separator bypass to production due to measurement at the de-gassing station". During all periods where rates were not recorded, these where instead extrapolated. Back allocated daily production rates exist from the date the well began production, and these were used to complete the production history prior to the start of flow testing.

Table D-1: Well R1 fluid data

Field	Value	Units	Source
Oil Gravity	26	deg api	Well testing report
GOR	290	scf/stb	Well testing report
Volume Factor	1.4	-	Field Development Plan
Viscosity	0.71	cp	PVT analysis
Oil Compressibility	1.13E-5	1/psi	Reservoir simulation model
Water Compressibility	3.1E-6	1/psi	Reservoir simulation model

Table D-2: Well R1 reservoir and well data

Field	Value	Units	Source
Porosity	16.7	%	Petrophysical logs
Water Saturation	15.7	%	Petrophysical logs
Net Thickness	31.5	ft	Petrophysical logs
Rock Compressibility	1E-6	1/psi	Typical Values
Wellbore Radius	0.2917	ft	Completion report
Perforated thickness	24	ft	Completion report + petrophysics logs. Perforated interval x Net to Gross for zone.
Reservoir Temperature	214	deg f	Well testing downhole gauge measurement
Reservoir Pressure	4153	psi	Well testing downhole gauge measurement at end of shut in

Appendix E: Well R2 Data Quality Check and Static Data

Well R2 was subject to flow performance tests over a period of 41.8 hours. During this period the well was shut in for 21.05 hours. A PLT string with a single gauge was used for pressure measurements. This was lowered during a static pass, and parked at reservoir depth capturing the build-up and preceding drawdown. Examination of the pressure data showed that it exhibited 4 distinct spikes (Table E-1). These have been attributed to poor data collection, possibly caused by maintenance to the generator. To counter these data quality issues, a derivative smoothing factor of 5% was used.

Table E-1: Well R2 data quality analysis, summary of pressure spikes

Time	Duration	Amplitude
18 Oct 2011 19:58	7s	1.1 psi
18 Oct 2011 21:20	7s	2.2psi
18 Oct 2011 22:16	7s	2.1psi
19 Oct 2011 13:36	8s	1.1psi

Rate data from the flow test was used where available. The test package was bypassed overnight with the well flowing directly to the production pipeline, preventing rate readings from being captured. Back allocated daily production rates exist from the date the well began production, and these were used to complete the production history prior to the start of flow testing. Fig. E-1 highlights the need for using a full rate history by showing that a 60 hour truncated rate history causes significant derivative end effects.

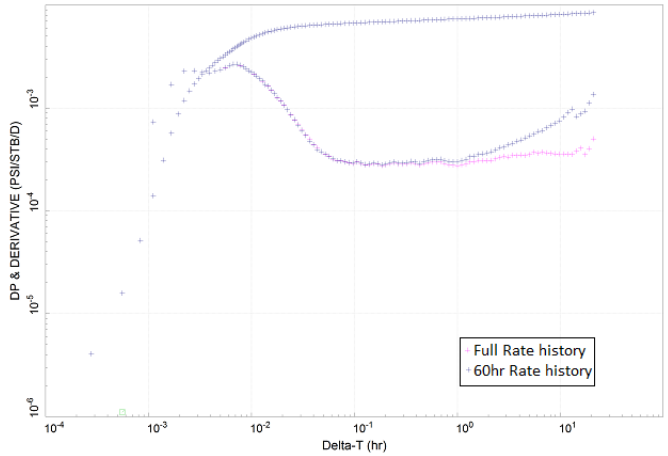

Fig. E-1: Derivative End Effects

Table E-2: Well R2 fluid data

Field	Value	Units	Source
Oil Gravity	31.7	deg api	Well testing report
GOR	719	scf/stb	Well testing report
Volume Factor	1.4	-	Field Development Plan
Viscosity	0.71	cp	PVT analysis
Oil Compressibility	1.13E-5	1/psi	Reservoir simulation model
Water Compressibility	3.1E-6	1/psi	Reservoir simulation model

Table E-3: Well R2 reservoir and well data

Field	Value	Units	Source
Porosity	18.94	%	Petrophysical logs
Water Saturation	5.67	%	Petrophysical logs
Net Thickness	181.5	ft	Petrophysical logs
Rock Compressibility	1E-6	1/psi	Typical Values
Wellbore Radius	0.2917	ft	Completion report
Perforated thickness	138.43	ft	Completion report + petrophysics logs
Reservoir Temperature	201	deg f	Well testing downhole gauge measurement

Appendix F: Well M1 Data Quality Check and Static Data

Well M1is a producer situated in the north of the northern dome, and is perforated in The Limestone. The shut in used for PTA dates from 1974, and took place after the well tubing was pulled following an acid job during which the wire-line tools were lost due to a wire breakage.

Well M1 was flowed at a rate of 14900 bpd for a period of 7 days before being shut in. As the less prolific reservoir, PTA data from The Limestone is scarce, and the age of this data results in two constraints. Firstly, the sampling period of 1 minute in the early time makes it difficult to assess when wellbore storage ends through derivative analysis. Secondly, the pressure gauge resolution does not allow detection of the small pressure changes which occur towards the end of the PBU. As a result of this second constraint, only 40 hours of the 65 hour build-up have been included in the analysis.

Table F-1: Well M1 fluid data

Field	Value	Units	Source
Oil Gravity	28.24	deg api	Analysis report
Volume Factor	1.322	-	Well testing report
Viscosity	1.72	cp	Well testing report
Oil Compressibility	6.638E-6	1/psi	Well testing report
Water Compressibility	3E-6	1/psi	Typical Values

Table F-2: Well M1 reservoir and well data

Field	Value	Units	Source
Porosity	18	%	Well testing report
Water Saturation	9.32	%	Analysis report
Net Thickness	347.2	ft	Well testing report
Rock Compressibility	1E-6	1/psi	Typical Values
Wellbore Radius	0.229	ft	Well testing report
Perforated thickness	312	ft	Well testing report
Reservoir Pressure	3687	psi	Well testing report

Table F-3: Well M1 historic interpretation

Field	Value	Units	Source
Permeability	173.1	mD	Well testing report
Skin	0.777	-	Well testing report

Appendix G: Well M2 Data Quality Check and Static Data

Well M2 is an injector situated at the crest of the northern dome, and is perforated in The Limestone. The well was completed in 1984, and has been periodically used for trial injection since. The shut in used for PTA was performed to assess the results of an acid job which was conducted on Well M2.

Well M2 was used to perform injection water pumping with rates of 8640 bpd for a period of 4 hours. before pumping ceased due to pump issues. Pumping commenced the following day with a rate of 8350-9100bbl/min (c 2600psi) for a period of 12 hours. Pumping then ceased for a period of 24 hours. Two memory gauges were used recorded both build-ups. Gauge 2, having been more recently calibrated, was used in the PTA.

Table G-1: Well M2 fluid data

Field	Value	Units	Source
Volume Factor	1	-	Water injection
Oil Viscosity	1.32	cp	Depletion Plan
Water Viscosity	0.6	cp	Water Injection
Oil Compressibility	6.64E-6	1/psi	Well testing report for M1
Water Compressibility	3E-6	1/psi	Typical Values

Table G-2: Well M2 reservoir and well data

Field	Value	Units	Source
Porosity	12	%	Reservoir Engineering model
Water Saturation (Outer)	14	%	Reservoir Engineering model
Water Saturation (Inner)	100	%	Water injection
Net Thickness	137.8	ft	Completion report
Rock Compressibility	1E-6	1/psi	Typical Values
Wellbore Radius	0.2917	ft	Completion report
Perforated thickness	137.8	ft	Completion report
Reservoir Temperature	104	deg f	Well testing downhole gauge measurement
Reservoir Pressure	4200	psi	Well testing downhole gauge measurement at end of shut in

Appendix H: Design Application for Pressure Transient Analysis (DAPTA)

DAPTA allows engineers to rapidly establish the optimum shut-in period for a well by providing estimates of a) time until wellbore storage ends, b) time until radial flow begins, and c) radius of investigation. DAPTA is validated by comparing the estimates produced with actual test data obtained from six wells in a giant Middle Eastern field. This field was chosen to allow validation with both producers and injectors, across sandstone and carbonate reservoirs with ranges of permeability and skin.

DAPTA was designed with the objective of simplifying the design of Pressure Transient Analysis (PTA) campaigns for engineers. It takes industry accepted methods, and presents them using an intuitive, easy to follow Graphical User Interface (GUI). It allows users to provide inputs using the most common units for each parameter. Users are presented with all formulas and type-curves used through the GUI. This aims to facilitate fully informed engineering decisions, and eliminate the confusion which often arises from more advanced software packages.

To simplify data input and output DAPTA stores all parameters within a Microsoft Excel spreadsheet. DAPTA was created using the Visual Basic for Applications programing language, with the GUI being designed with UserForms.

Wellbore Storage Constant

The concept of wellbore storage was first introduced (van Everdingen and Hurst, 1949) as "the volume of fluid unloaded from the annulus per second, corrected to reservoir conditions" (H-1).

$$q_{A(t)} = C\frac{d\Delta p}{dt} \quad \text{(H-1)}$$

Ramey (1965) used this equation to define the liquid loading wellbore storage, i.e. the volume of fluid produced from the annulus when a well is opened to flow, and the fluid expansion wellbore storage, i.e. the volume of fluid produced due to expansion ((H-2 and H-3 respectively).

$$C_{LL} = \frac{V_u}{\left(\frac{\rho}{144}\frac{g}{g_c}\right)} \quad \text{(H-2)}$$

$$C_{FE} = c_{well}.V_{well} \quad \text{(H-3)}$$

Fig. H-1 shows a screenshot of the DAPTA Wellbore Storage (WBS) calculator which includes four options for calculating wellbore storage, the parameters for each being provided by the user:

1. Liquid Level Annulus – The casing inner-diameter is used to calculate wellbore volume per unit length, V_u. The user provides either oil density (lb_m/ft^3) or oil gravity (degrees API). Eq. (H-2 is then used to calculate the wellbore storage.
2. Liquid Level Packer – The tubing inner-diameter is used to calculate V_u. The user provides either oil density (lb_m/ft^3) or oil gravity (degrees API). Eq. (H-2 is then used to calculate the wellbore storage.
3. Fluid Expansion Annulus – The casing inner-diameter and well depth are used to calculate the total wellbore volume. Eq. H-3 is then used to calculate the wellbore storage.
4. Fluid Expansion Packer – The tubing inner-diameter, packer depth, casing inner-diameter and well depth are used to calculate wellbore volume. Eq. H-3 is then used to calculate the wellbore storage.

The oil and gas wellbore storage constant is made dimensionless using Eq. H-4 (Ramey, 1965), with the total formation compressibility term c_t being found through Eq. H-5 which assumes the field is operated above the bubble point.

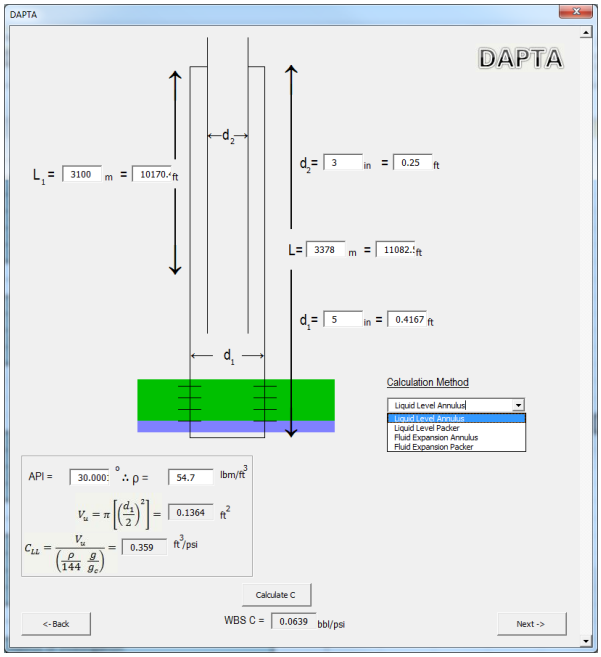

Fig. H-1: Screenshot of DAPTA wellbore storage calculator

$$C_D = \frac{0.8936C}{\phi c_t h\, r_w^2} \quad \text{(H-4)}$$

$$c_{Total} = c_{Oil}(1 - S_W) + c_{Water}(S_W) + c_{Rock} \quad \text{(H-5)}$$

Type Curve Parameter

A type-curve which plots dimensionless pressure P_D (H-6) on the y-axis against dimensionless time t_D (H-7) was published by Agarwal, Al-Hussainy and Ramey (1970). This was developed into a new type-curve which plots P_D against t_D/C_D, with each curve being characterised by a value of C_De^{2s} (Gringarten *et al.*, 1979). In both cases, the curves were constructed through a Laplace domain analytical solution to the diffusivity equation for a constant rate drawdown in a finite radius well, with infinitesimal skin, positioned in an infinite reservoir ((H-8). This is inverted in DAPTA through use of the Gaver-Stehfest algorithm in Eq. H-9 (Gaver, 1966 and Stehfest, 1970).

$$p_D = \frac{kh\,\Delta p}{141.2qB\mu} \quad \text{(H-6)}$$

$$t_D = \frac{0.000264kt}{\phi\mu c_t r_w^2} \quad \text{(H-7)}$$

$$L\{P_D\} = \frac{K_0(\sqrt{s}) + S\sqrt{s}.K_1(\sqrt{s})}{2s\left\{\sqrt{s}\,.K_1(\sqrt{s}) + C_D.s\left[K_0(\sqrt{s}) + S\sqrt{s.K_1(\sqrt{s})}\right]\right\}} \quad \text{(H-8)}$$

$$Fa(L\{P\}) = \frac{ln2}{t}\sum_{i=1}^{N} V_i P\left(\frac{ln2}{t}\, i\right);\ where\ V_i(N) = (-1)^{\frac{N}{2}+i}\sum_{k=\frac{i+1}{2}}^{min(i,\frac{N}{2})} \frac{k^{\frac{N}{2}}(2k)!}{\left(\frac{N}{2}-k\right)!k!(k-1)!(i-k)!(2k-1)!} \quad \text{(H-9)}$$

DAPTA requires an estimate of skin to find C_De^{2S} and for use in Eq.**Error! Reference source not found.**. Since an accurate value of skin can only be known following the conclusion of PTA, estimating this may present a challenge. Knowledge of the well completion and values of skin from earlier analysis can be used to develop this estimate. It is important that users avoid conservative estimates to prevent flow regime time limits being underestimated.

Using Eq.7 and Eq.8, DAPTA produces the Gringarten type-curve (Gringarten *et al.*, 1979) for values of t_D/C_D between 1E-1 and 1E5, and C_De^{2s} between 1E-3 and 1E60 (**Error! Reference source not found.**, white). Negative values of skin are approximated by evaluating the equation with no skin, and accounting for the effective wellbore radius using the substitutions in Eq. (H-10. Using the value of dimensionless wellbore storage calculated, and the value of skin provided by the user, the type curve is then plotted (Fig. H-3, orange).

$$t'_D = t_D e^{2s}; \quad C'_D = C_D e^{2s} \quad \text{(H-10)}$$

End of Wellbore Storage

Wellbore storage on a Gringarten type curve corresponds to an early time unit slope, indicating $P_D = t_D/C_D$. Gringarten *et al.* (1979) suggested that a 5% "Approximation Percentage" is suitable for finding the limit of this flow regime for practical applications. Essentially this implies that wellbore storage can be assumed to end when the derivatives deviates from the unit slope by 5%. Data collected from a giant Middle Eastern oil field suggest that an Approximation Percentage of 10% is more appropriate for use in DAPTA. Changes to this parameter are only recommended if backed by empirical data such as that discussed later in this paper.

DAPTA finds the end of wellbore storage by iteratively evaluating the dimensionless pressure at 100 points per logarithmic cycle, and finding the point at which it deviates from the unit slope by greater than the Approximation Percentage provided (Fig. H-2).

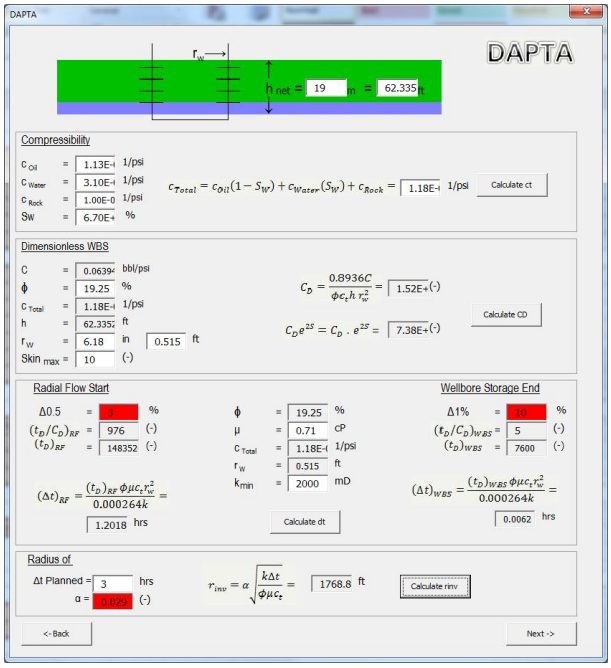

Fig. H-2: Screenshot of DAPTA flow regime calculator

Start of Radial Flow

During radial flow, the dimensionless pressure can be approximated by Eq. H-11. Bourdet *et al.* (1983) developed the derivative type-curve which superimposed the Gringarten type curve with a derivative group (H-12). This type curve was built on the basis that radial flow can be assessed by evaluating the derivative of test data and comparing it to the derivative of H-11 $(t_D/C_D)\frac{d(P_D)}{d(t_D/C_D)} = 0.5$ (Bourdet and Gringarten, 1980).

The type curve authors suggested that a 10% Approximation Percentage provides an adequate indication of radial flow. Data collected from a giant Middle Eastern oil field suggests that an Approximation Percentage of 3% is more appropriate for use in DAPTA, as this ensures a sufficient margin for error in the optimum test duration. Changes to this parameter are only recommended if backed by empirical data such as that discussed later in this paper.

$$P_D = \frac{1}{2}(ln\frac{t_D}{C_D} + 0.80907 + C_D e^{2S}) \quad \text{(H-11)}$$

$$\left(\frac{t_D}{C_D}\right)\frac{d(P_D)}{d\left(\frac{t_D}{C_D}\right)} \quad \text{(H-12)}$$

DAPTA plots the derivative type curve using the same method discussed for plotting of the Gringarten type curve. The beginning of radial flow is estimated by iteratively evaluating the derivative at 100 points per logarithmic cycle. When the type curve converges with the derivative stabilisation, $P_D' = 0.5$ by an amount equal to the Approximation Percentage, radial flow is reported as having occurred (Fig. H-3).

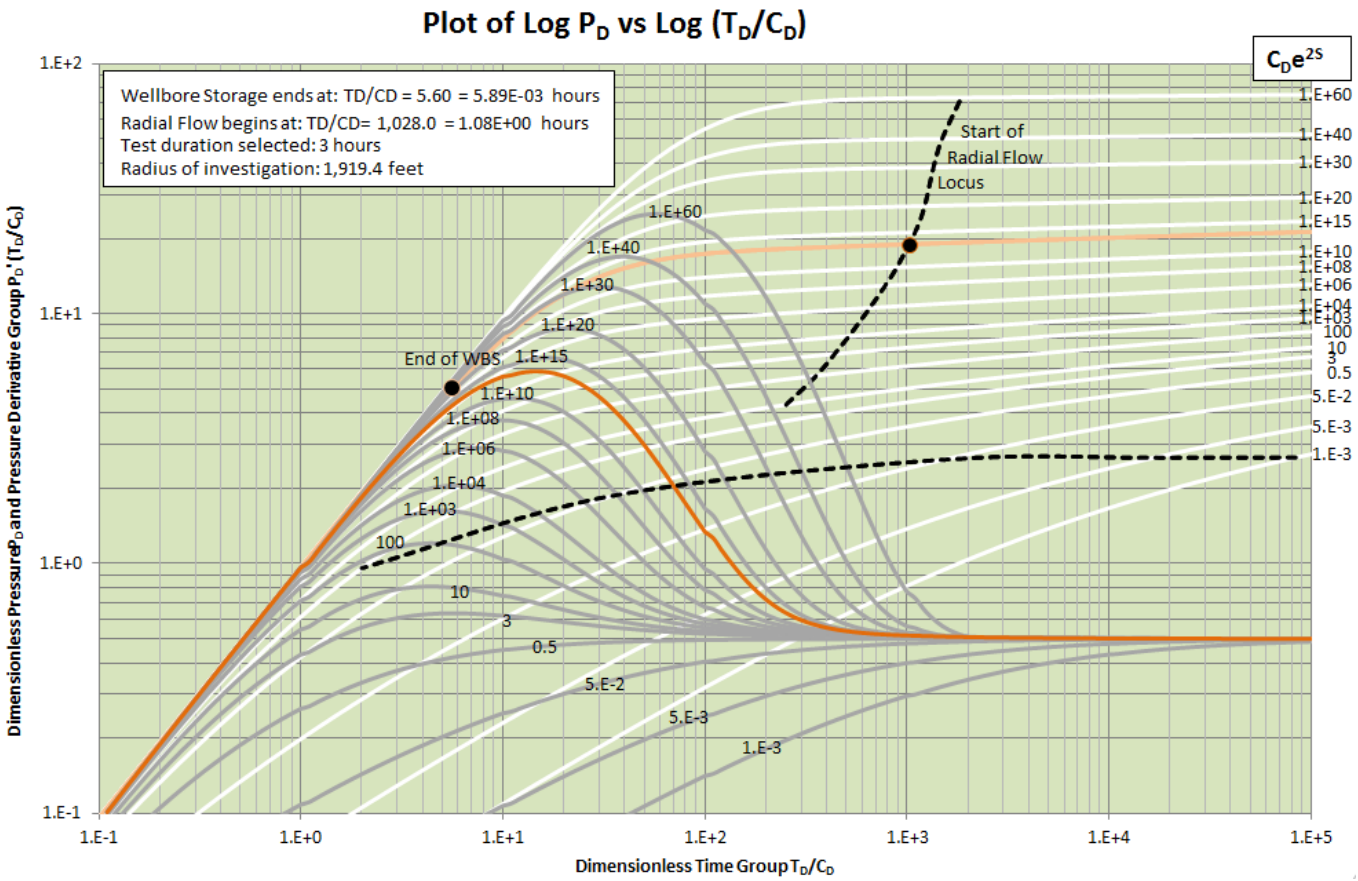

Fig. H-3: Screenshot of the type curve generated by DAPTA

Radius of Investigation

As a pressure transient moves through the reservoir, it provides information about the formation traversed. The radius of investigation (H-13) provides an indication of how far a transient has travelled into a formation, assuming a vertical well in an infinite acting homogeneous reservoir with normal (0.1psi) pressure gauge resolution (van Poollen, 1964). This is useful in assessing the required PTA duration, especially when the objective is delineation of known geological features or appraisal of new reservoirs. DAPTA uses this equation together with the chosen test duration provided by the user to calculate a radius of investigation for the test. The user is encouraged to ensure the test duration chosen is sufficiently greater than the estimate of time until radial flow reported by DAPTA.

$$r_{inv} = 0.029\sqrt{\frac{k\Delta t}{\phi\mu c_t}} \quad \text{(H-13)}$$

DAPTA Verification Using Test Data

DAPTA has been primarily validated using data from a giant Middle Eastern field. The estimates generated by DAPTA have been compared with existing pressure transient data to optimise the Approximation Percentages already discussed. This was performed by fully analysing each set of pressure transient data using derivative analysis (see main paper) in one of the conventional well test interpretation software packages (PIE). The reported end of wellbore storage and start of radial flow were then compared to the estimates from DAPTA.

Error! Reference source not found. shows a comparison of the flow regime time limits calculated using derivative analysis, and using DAPTA for each of the six wells considered. This shows that generally the time limit predictions from DAPTA using Approximation Percentages of 10% for wellbore storage ending, and 3% and for radial flow beginning conform reasonably to those found through derivative analysis. The one notable exception is well M2; where radial flow is predicted to begin much later than it actually does. This would lead to the optimum test duration being overestimated. While this is not ideal, it would not lead to an inaccurate PTA and is preferable to an underestimate. This is hence deemed acceptable.

Table H-1: Summary of comparison for all wells verified

	End of Wellbore Storage		Start of Radial Flow	
	Derivative Analysis	**DAPTA**	**Derivative Analysis**	**DAPTA**
Well U1	3	3	1000	1000
Well U2	5	3.4	1000	880
Well R1	6	4.2	800	1000
Well R2	4	4.7	600	936
Well M1	/	1.9	300	564
Well M2	/	0.03	30	135